Published for SISSA by Springer

Received: *March 28, 2022*
Accepted: *July 5, 2022*
Published: *September 27, 2022*

Analytic expansions of multi-hadron finite-volume energies. I. Two-particle states

D. M. Grabowska[a] **and M. T. Hansen**[b]

[a] *Theoretical Physics Department, CERN, 1211 Geneva 23, Switzerland*
[b] *Higgs Centre for Theoretical Physics, School of Physics and Astronomy, The University of Edinburgh, Edinburgh EH9 3FD, U.K.*

E-mail: dorota.grabowska@cern.ch, maxwell.hansen@ed.ac.uk

Abstract: We derive analytic expansions for the finite-volume energies of weakly-interacting two-particle systems, using the general relations between scattering amplitudes and energies derived by Lüscher and others. The relations hold for ground and excited states with both zero and non-zero total momentum in the finite-volume frame. A number of instructive aspects arise in the derivation, including the role of accidental degeneracies and the importance of defining a power-counting scheme in the expansions. The results give intuition concerning the imprint of perturbative interactions on the energy spectrum, while also providing a useful basis for the analogous results concerning three-particle excited states, to appear. We have also developed a Mathematica notebook that automates the expansions described in this work.

Keywords: Algorithms and Theoretical Developments, Hadronic Spectroscopy, Structure and Interactions, Lattice QCD

ArXiv ePrint: 2110.06878

https://doi.org/10.1007/JHEP09(2022)232

JHEP09(2022)232

Contents

JHEP09(2022)232

1 Introduction

An overwhelming body of evidence has established quantum chromodynamics (QCD) as a precise and quantitative description of the strong nuclear force over an incredible range of energies. However, due to a mismatch between the fundamental fields of the theory (quarks and gluons) and the low-energy degrees of freedom (bound states of quarks and gluons, called hadrons), extracting first-principles predictions can be challenging. This is especially true for moderate-energy multi-hadron processes, for which both low-energy effective theory and high-energy perturbative methods break down.

Lattice QCD is a proven method for reliably determining the properties of QCD, especially where analytic techniques fail, by making use of Monte Carlo importance sampling to numerically estimate the quantum path integral, regulated via discretization on a finite spacetime grid. This method has reached an era of sub-percent precision for many single-hadron quantities and has also proven reliable in extracting more complicated, two-hadron

observables. Examples in the latter category include two-meson, meson-baryon and baryon-baryon scattering amplitudes as well as one-to-two decay and transition amplitudes. See refs. [1–6] for recent reviews. More recently, the reach of these calculations has extended to three-to-three scattering amplitudes. See refs. [7–9] for reviews of the progress in this sector.

The standard methodology in the majority of multi-hadron calculations is to use the finite system size of the calculation (the finite volume) as a tool in probing physical observables. In particular, when the fields are constrained to have periodicity L in the three spatial directions, then the continuum of multi-hadron energies is replaced with a discrete set, denoted $E_n(L)$. One can then use field theoretic methods to relate the values of these energies to scattering amplitudes. A modern, rigorous, and general formulation of this idea was provided by Lüscher in refs. [10, 11], in which he related the two-to-two elastic scattering amplitude of identical spin-zero particles to finite-volume energies with vanishing total spatial momentum, $\boldsymbol{P} = \boldsymbol{0}$, in the finite-volume frame. This has since been generalized to include non-zero momentum, multiple two-particle channels of non-identical and non-degenerate particles, as well as particles with non-zero spin [12–21]. Most recently, the methods have been extended to the extraction of amplitudes involving three hadrons in either the initial or final state [22–39].

The purpose of this work, together with a second article to appear, is to derive analytic relations for two- and three-particle finite-volume energies of weakly interacting systems, in the low-energy regime for which only a single channel of identical scalar or pseudo-scalar particles can propagate. The results are directly applicable, for example, to maximal isospin multi-pion and multi-kaon channels is QCD, as well as other weakly-interacting multi-boson systems, including calculations of non-QCD lattice field theories. The present work focuses on two-particle states and extends previous derivations by providing expansions for ground and excited-state energies with any value of total momentum $\boldsymbol{P}$ in the finite-volume frame as well as describing the contribution of all angular momentum components.

The general relation between energies and scattering amplitudes, restricted to the regime of a single two-particle channel, can be packaged into a single master-function, depending on the energy E, the total three-momentum in the finite-volume frame $\boldsymbol{P}$, and the volume L, as well as the scattering amplitude across all partial waves ℓ, denoted $\mathcal{M}_\ell$, and the specified irreducible representation (irrep) of the finite-volume energies of interest. The latter is defined with respect to the symmetry group of the system, either the full octahedral group including parity or the little group thereof that leaves $\boldsymbol{P}$ invariant. The function is constructed such that its roots in E, with all other inputs held fixed, give the discrete finite-volume spectrum $E_n(L)$ of the system. The condition that this function should vanish is referred to as a quantization condition. To make use of the relations in practice, one must generally truncate the system by approximating $\mathcal{M}_\ell = 0$ for $\ell > \ell_{\mathsf{max}}$. This work considers both the case of S-wave dominance, for which $\ell_{\mathsf{max}} = 0$, as well as the effects of higher partial waves, detailed in sections 2.5 and 2.6. As described in section 2.5, it is even possible to write the leading contribution from all partial waves in a compact form. (See also ref. [10].)

As we discuss extensively in section 2.6, special care must be taken care for the so-called accidentally degenerate states, already discussed in refs. [10, 40, 41]. To define these, note

JHEP09(2022)232

that a theory of two non-interacting particles in a periodic cubic volume of length L, is characterized by assigning a momentum to each, quantized as an integer-vector multiple of $2\pi/L$. For $\boldsymbol{P} = \mathbf{0}$ the two momenta are back-to-back so that a single three-vector characterizes the state. In this case the first accidentally degenerate state is the 8^{th} excited state, for which non-interacting pions can have back-to-back momentum of type $(0, 0, 3)$ or else of type $(1, 2, 2)$. In section 2.6, we describe such states in detail, for various values of $\boldsymbol{P}$, and discuss the role higher angular momenta in breaking the degeneracy.

In addition to providing the basis for our subsequent work on three-particle states, we envision a number of broader applications for the results presented here. These include

- Building general intuition on the interaction-induced shifts to finite-volume energies,
- Better understanding cancellations leading to exponentially suppressed volume effects in correlators, given the power-like volume dependence of energies in their spectral decompositions,
- Guiding automated root finders of the full two-particle quantization condition,
- Exploring the convergence of contributions from higher-partial waves to finite-volume energies.

The question of how the value of $E_n(L)$ converges as a function of ℓ_{max} has also recently been studied in ref. [42]. We comment in more detail on each of these points in the conclusion.

We emphasize that the results presented here hold only in the energy regime where the system is weakly interacting and break down, for example, in the vicinity of a narrow resonance. However, even in a resonant system, the expansion will give a good description for any fixed state at sufficiently large L. This is because the physical energy of a given state decreases with increasing L, eventually moving away from the resonant behavior and closer to threshold. An exception to the general validity for large L is systems at unitarity, for which the scattering amplitude has a pole at threshold.

It is important to put this work in context of previously published results concerning expansions of finite-volume energies for weakly-interacting systems. Already in refs. [10, 11], Lüscher considered the large-volume expansion of both the ground state and excited states without accidental degeneracy, for $\boldsymbol{P} = \mathbf{0}$. The ground-state result matched earlier work of Huang and Yang [43], who gave an expression for any number of particles, focusing on the special case of non-relativistic hard spheres. This was later generalized and re-derived in various contexts in refs. [44–48], leading to a result for the ground-state finite-volume energy of any number of relativistic bosons. More recently, an expansion of three-particle excited states has been presented in refs. [49, 50]. Finally, in ref. [41], Luu and Savage provide an extensive exploration of the phenomenology of Lüscher's quantization condition, including detailed discussion of the finite-volume symmetry group, the role of accidental degeneracies and prospects for extracting higher angular-momentum components from numerical lattice calculations.

This work differs from the results summarized above in three key ways. First we argue that the expansion for excited states is non-unique and can only be performed in the

JHEP09(2022)232

context of a particular power-counting scheme. The latter should be defined to give the best description of the exact energy for a given set of scattering parameters. In particular, we argue that the large-volume expansion is misleading in the sense that L dependence arises in various kinematic factors, including the Lorentz boost factor and the non-interacting energy. Re-expanding these about infinite L is required to recover certain earlier results, but for excited states we find this degrades the descriptive power without simplifying the results and is not needed. Second, we give a more general framework for covering a wide-range of cases including the contribution of any number of partial waves in the expansion and the general strategy for treating accidentally degenerate states. Third and finally we give results for the ground and excited state expansions for nonzero $\boldsymbol{P}$ that, as far as we know, have not been considered previously. This is of particular importance as it is a crucial input for the corresponding expansions of three-particle energies considered in the companion manuscript, to appear.

The remainder of this work is organized as follows: in the next section we derive the general expansion of two-particle states with any momentum $\boldsymbol{P}$ in the finite-volume frame, taking particular care to establish a general notation, to specify the role and non-uniqueness of power-counting schemes in defining the expansion, and to explore the effects of higher partial waves, including the case of accidental degeneracy. The main concrete results of this work are summarized in eqs. (2.21), (2.39), (2.54), in tables 4–8, and in the discussion of section 2.6. Then, in section 3, we describe various numerical checks performed by comparing our expansion to the general solutions of the quantization condition, as well as summarizing the Mathematica [51] notebook, available at ref. [52], that can be used to automate higher order expansions. In section 4 we briefly conclude. This work additionally contains five appendices, addressing more technical aspects of the derivation including a description of the finite-volume functions required for the quantization condition, a comment on energy level crossings, a summary of the relevant symmetry groups and projectors, and an important relation concerning non-interacting energies, required to perform the expansion.

2 Derivation and results

The following subsections review the general formalism and establish the expansion strategy and the notation used. The main results are emphasized at the end of each subsection.

2.1 Set-up

Our aim is to perturbatively expand finite-volume two-particle energies, collectively denoted $E_{n,\boldsymbol{P},\Lambda}(L)$, about the non-interacting limit. Here the integer index n indicates the n^{th} excited state ($n = 0$ the ground state), $\boldsymbol{P}$ is the total spatial momentum of the two-particle system, Λ is the relevant finite-volume irrep, and L is the box length. The total momentum $\boldsymbol{P}$ is equal to an integer-vector multiple of $(2\pi/L)$. We write this as $\boldsymbol{P} = (2\pi/L)\boldsymbol{d} = (2\pi/L)(d_x, d_y, d_z)$ and use the shorthand $\boldsymbol{P} = [d_x d_y d_z]$. In this work we restrict attention to a single channel of identical scalar particles with mass m.

The simplest example of the expressions derived in this work is that of the two-particle ground state ($n = 0$) for vanishing spatial momenta $\boldsymbol{P} = [000]$ in the trivial-irrep $\Lambda = A_{1g}$

JHEP09(2022)232

of the octahedral group O_h. The result, through $\mathcal{O}(1/L^5)$, was presented by Huang and Yang in ref. [43] and subsequently extended to higher orders. In our notation the first non-trivial order reads

$$E_{0,[000],A_{1g}}(L) = 2m + \frac{4\pi a_0}{mL^3} + \mathcal{O}\left(1/L^4\right) , \tag{2.1}$$

where a_0 is the two-particle scattering length, defined in eq. (2.33) below.

The key tool used to derive such results here is the finite-volume quantization condition [11, 12, 14]

$$\det_{\Lambda\mu}\Big[\mathbb{P}_{\Lambda,\mu}\cdot\Big[\mathcal{M}(E^\star)^{-1} + F(E,\boldsymbol{P},L)\Big]\cdot\mathbb{P}_{\Lambda,\mu}\Big]\Big|_{E=E_{n,\boldsymbol{P},\Lambda}(L)} = 0\,, \tag{2.2}$$

where $\mathcal{M}(E^\star)$ is the infinite-volume scattering amplitude and F is a matrix of known geometric functions, reviewed in appendix A. The matrix F depends on the total energy and momentum in the finite-volume frame, $(E,\boldsymbol{P})$, as well as the box length, L. By contrast, the scattering amplitude only depends on the center-of-momentum frame (CoM frame) energy

$$E^\star = \sqrt{E^2 - \boldsymbol{P}^2}\,. \tag{2.3}$$

We have also introduced $\mathbb{P}_{\Lambda,\mu}$ as a projector restricting to the irrep of interest. Some discussion of finite-volume groups and projectors is included in appendix C. See also refs. [11, 12, 53, 54] for more details.

The matrices $\mathcal{M}(E^\star)$, $F(E,\boldsymbol{P},L)$ and $\mathbb{P}_{\Lambda,\mu}$ are each defined on an angular momentum space and carry two sets of spherical harmonic indices, e.g. $\mathcal{M}(E^\star) = \mathcal{M}_{\ell'm',\ell m}(E^\star)$ where $\ell = 0,1,2\cdots$ and $m = -\ell, -\ell+1, \cdots \ell$. The explicit definition can be given in terms of the ℓ^{th} scattering phase shift, δ_ℓ. In the case of a single channel of identical scalar (or pseudoscalar) particles, one has

$$\mathcal{M}_{\ell'm',\ell m}(E^\star) = \delta_{\ell'\ell}\delta_{m'm}\frac{16\pi E^\star}{p^\star}\frac{e^{2i\delta_\ell(p^\star)}-1}{2i} = \delta_{\ell'\ell}\delta_{m'm}\frac{16\pi E^\star}{p^\star\cot\delta_\ell(p^\star) - ip^\star}\,. \tag{2.4}$$

The scattering length a_0, appearing in eq. (2.1), is defined via the leading order expansion of $p^\star\cot\delta_0(p^\star)$ about threshold

$$p^\star\cot\delta_0\left(p^\star\right) = -\frac{1}{a_0} + \mathcal{O}\left(p^{\star 2}\right)\,. \tag{2.5}$$

Here we have also introduced the relative momentum

$$p^{\star 2} = \frac{E^{\star 2}}{4} - m^2\,. \tag{2.6}$$

See table 1 for a summary of the notation established so far, and continued in the following.

As the matrices are formally infinite dimensional, in practice one must truncate the quantization condition by setting $\mathcal{M}_{\ell'm',\ell m}(E^\star) = 0$ or equivalently $\delta_\ell(p^\star) = 0$ for $\ell > \ell_{\mathsf{max}}$. As discussed in refs. [10, 11, 14], one can then set the corresponding entries of F and $\mathbb{P}_{\Lambda,\mu}$ to

JHEP09(2022)232

Quantity	Definition/Key relation	Description
L	—	finite-volume box length
E	—	finite-volume-frame energy
n	—	level of the excited state
$\boldsymbol{P}$	$2\pi \boldsymbol{d}/L$	finite-volume-frame 3-momentum
$E^\star$	$\sqrt{E^2 - \boldsymbol{P}^2}$	center-of-momentum-frame energy
$\boldsymbol{k}$	$2\pi \boldsymbol{v}/L$	generic 3-momentum
ω_k	$\sqrt{\boldsymbol{k}^2 + m^2}$	on-shell time component of 4-vector k^μ
ℓm	indices on $Y_{\ell m}$	angular-momentum indices
$p^\star$	$\sqrt{E^{\star 2}/4 - m^2}$	relative momentum magnitude from $E^\star$
q	$Lp^\star/(2\pi)$	dimensionless version of $p^\star$
$\mathfrak{n}$	$\{n, \boldsymbol{P}, \Lambda\}$	collective index for a state $\mathfrak{n}$
$E_{\mathfrak{n}}^{(0)}(L)$	eq. (2.8)	non-interacting energy
$\boldsymbol{\nu}_{\mathfrak{n}}$	—	representative integer three-vector for state $\mathfrak{n}$
$q_{\mathfrak{n}}^{(0)2}$	$L^2[E_{\mathfrak{n}}^{(0)}(L) - \boldsymbol{P}^2 - 4m^2]/(2\pi)^2$	non-interacting dimensionless momentum
$\boldsymbol{S}_{\mathfrak{n}}$	eq. (2.15)	set of dimensionless momenta that give same non-interacting energy

Table 1. Summary of the notation used throughout the paper. Note that q is only used to denote the dimensionless momentum in the center-of-momentum (CoM) frame. We have dropped the $\star$, which generically indicates CoM quantities, for simplicity in this case.

zero without further approximation. Given a truncated version of eq. (2.2), the expansion is derived by substituting

$$E_{\mathfrak{n}}(L) = E_{\mathfrak{n}}^{(0)}(L) + \sum_{k=1}^{\infty} \epsilon^k \, \Delta_{E[\mathfrak{n}]}^{(k)}(L)\,, \tag{2.7}$$

where $\mathfrak{n} = \{n, \boldsymbol{P}, \Lambda\}$ is a collective index for all discrete information common to each building block and $E_{\mathfrak{n}}^{(0)}(L)$ is the finite-volume energy in the non-interacting limit, given e.g. by taking $\delta_\ell \to 0$ for all ℓ. This non-interacting energy can be written as

$$E_{\mathfrak{n}}^{(0)}(L) = \sqrt{m^2 + (2\pi/L)^2 \boldsymbol{\nu}_{\mathfrak{n}}^2} + \sqrt{m^2 + (2\pi/L)^2 (\boldsymbol{d} - \boldsymbol{\nu}_{\mathfrak{n}})^2}\,, \tag{2.8}$$

where $\boldsymbol{\nu}_{\mathfrak{n}}$ is an integer vector representing the non-interacting state. For most values of $\mathfrak{n}$, multiple choices of $\boldsymbol{\nu}_{\mathfrak{n}}$ are possible, so that this identifier is not unique. All quantities that depend on this vector, e.g. the non-interacting energy, $E_{\mathfrak{n}}^{(0)}(L)$, are equal for any valid choice. The correspondence between n and $\boldsymbol{\nu}_{\{n,\boldsymbol{P},\Lambda\}}$ is defined such that $E_{\mathfrak{n}}^{(0)}(L) < E_{\mathfrak{n}'}^{(0)}(L)$ for $n < n'$ *in the large* L *limit*. As we prove in appendix B, the sorting is independent of L in the CoM frame, but non-interacting level crossings can occur for non-zero total momenta.

Combining eqs. (2.2) and (2.7), it is possible to solve for the corrections $\Delta_{E[\mathfrak{n}]}^{(k)}$ order by order in terms of ϵ. As we explain in section 2.4 below, to completely define the expansion one must assign an epsilon scaling to various parameters entering $\mathcal{M}(E^\star)$ as well as, possibly

JHEP09(2022)232

(but not neccesarily), to $1/L$. There is no unique assignment and the best choice of power-counting scheme depends on the details of the system. Once a power-counting scheme is chosen, the iterative process of solving for the energy shifts can be automated; this is done in the Mathematica notebook accompanying this work [52]. See the end of section 3 for more details.

2.2 *S*-wave dominance: leading-order shift

We begin our explicit demonstrations with the expansion for the case of $\ell_{\text{max}} = 0$. For this truncation, only the trivial irreps (A_{1g} for $\boldsymbol{P} = [000]$ and A_1 otherwise) have finite-volume energies that are shifted by interactions. These are found by solving

$$p^\star \cot \delta_0(p^\star) = f(q, \boldsymbol{d}, L)\,, \tag{2.9}$$

where

$$f(q, \boldsymbol{d}, L) \equiv -16\pi E^\star \,\text{Re}\big[F_{00,00}(E, \boldsymbol{P}, L)\big] = -\lim_{s\to -1} \frac{1}{\gamma(q, \boldsymbol{d}, L)\,\pi L} \sum_{\boldsymbol{v}\in\mathbb{Z}^3} \Big[q^2 - \Gamma(\boldsymbol{v}|q, \boldsymbol{d}, L)\Big]^s . \tag{2.10}$$

The second equality is a standard definition of $F_{00,00}$, first introduced for nonzero $\boldsymbol{d}$ in ref. [12], and the limit indicates that the sum is regulated by analytically continuing from $\text{Re}[s] < -1$ [11]. The relation between this and other standard definitions, and the corresponding expressions for general $F_{\ell' m', \ell m}(E, \boldsymbol{P}, L)$, are reviewed in appendix A. In eq. (2.10) we have also adjusted the coordinate dependence, changing from $E, \boldsymbol{P}, L$ to $q, \boldsymbol{d}, L$, with the latter including

$$q^2 = \left(\frac{L}{2\pi}\right)^2 \left(\frac{E^2}{4} - \frac{\boldsymbol{P}^2}{4} - m^2\right), \qquad \gamma(q, \boldsymbol{d}, L) = \left[1 + \frac{\boldsymbol{d}^2}{4(q^2 + [mL/(2\pi)]^2)}\right]^{1/2}. \tag{2.11}$$

As is summarized in table 1, q is proportional to $p^\star$, made dimensionless by $L/(2\pi)$. Although we generically use a $\star$ superscript to denote CoM frame quantities, we drop this for q to avoid over-cluttering the notation in the following. The quantity $f(q, \boldsymbol{d}, L)$ also depends on

$$\Gamma(\boldsymbol{v}|q, \boldsymbol{d}, L) \equiv \frac{1}{\gamma(q, \boldsymbol{d}, L)^2} \left(\frac{\boldsymbol{v}\cdot\boldsymbol{d}}{|\boldsymbol{d}|} - \frac{|\boldsymbol{d}|}{2}\right)^2 + \left(\frac{\boldsymbol{v}\cdot\boldsymbol{d}}{|\boldsymbol{d}|^2}\,\boldsymbol{d} - \boldsymbol{v}\right)^2, \tag{2.12}$$

denoted by r^2 in ref. [12].

Since both the left- and the right-hand sides of eq. (2.9) are analytic functions of q^2, it is easiest to use this quantity in the expansion. We therefore define $q_{\mathfrak{n}}(L)^2$ by evaluating eq. (2.11) at $E_{\mathfrak{n}}(L)$ and also introduce the analog of eq. (2.7) above

$$q_{\mathfrak{n}}(L)^2 = q_{\mathfrak{n}}^{(0)}(L)^2 + \sum_{k=1}^{\infty} \epsilon^k\, \Delta^{(k)}_{q[\mathfrak{n}]}(L)\,. \tag{2.13}$$

Here $q_{\mathfrak{n}}^{(0)}(L)^2$ is the non-interacting version of $q_{\mathfrak{n}}(L)^2$, defined by evaluating eq. (2.11) at $E_{\mathfrak{n}}^{(0)}(L)$.

Having introduced all notation, the general procedure is relatively straightforward: evaluate both sides of eq. (2.9) at $q_{\mathfrak{n}}(L)^2$ and solve the equation order-by-order ϵ to determine

JHEP09(2022)232

n	$\boldsymbol{P}$	Λ	$\boldsymbol{S}_{\mathfrak{n}}$	$g_{\mathfrak{n}}$
0	[000]	A_{1g}	$(0,0,0)$	1
1	[000]	A_{1g}	$(0,0,1)$ + rotations and flips	6
8	[000]	A_{1g}	$(1,2,2)$ + rotations and flips (24 total) $(0,0,3)$ + rotations and flips (6 total)	30
0	[001]	A_1	$(0,0,0)$, $(0,0,1)$	2
1	[011]	A_1	$(0,0,1)$, $(0,1,0)$	2
0	[002]	A_1	$(0,0,1)$	1

Table 2. Examples for the set $\boldsymbol{S}_{\mathfrak{n}}$ with total number of elements $g_{\mathfrak{n}}$. In the accidentally degenerate case, $n = 8$ and $\boldsymbol{P} = [000]$, all three-vectors satisfying eq. (2.15) are included in the definition.

$\Delta^{(k)}_{q[\mathfrak{n}]}(L)$. If desired, the result can then be readily converted back to $E_{\mathfrak{n}}(L)$, which can be re-expanded to fixed order in ϵ.

To begin this iterative procedure, we take $p^\star \cot \delta_0(p^\star) = \mathcal{O}(1/\epsilon)$ and infer that the leading-order constraint arising from eq. (2.9) is that $f(q_{\mathfrak{n}}, \boldsymbol{d}, L)$ must also scale as $1/\epsilon$. This is achieved by requiring

$$q^{(0)}_{\mathfrak{n}}(L)^2 - \Gamma\left(\boldsymbol{v}|q^{(0)}_{\mathfrak{n}}, \boldsymbol{d}, L\right) = 0\,. \tag{2.14}$$

As was first shown in refs. [12, 14] and as we review in appendix D this is consistent with the relation between $q^{(0)}_{\mathfrak{n}}(L)^2$ and $E^{(0)}_{\mathfrak{n}}(L)$ and with eq. (2.8).

To expand beyond the trivial order, we define $\boldsymbol{S}_{\mathfrak{n}}$ as the set of all integer three-vectors $\boldsymbol{v}$ satisfying eq. (2.14), equivalently

$$\boldsymbol{S}_{\mathfrak{n}} = \left\{ \boldsymbol{v} \in \mathbb{Z}^3 \;\middle|\; E^{(0)}_{\mathfrak{n}}(L) = \sqrt{m^2 + (2\pi/L)^2 \boldsymbol{v}^2} + \sqrt{m^2 + (2\pi/L)^2 (\boldsymbol{d} - \boldsymbol{v})^2} \right\}. \tag{2.15}$$

In general, $\boldsymbol{S}_{\mathfrak{n}}$ is given by all rotations of both $\boldsymbol{\nu}_{\mathfrak{n}}$ and $\boldsymbol{d} - \boldsymbol{\nu}_{\mathfrak{n}}$ by elements of the little group of $\boldsymbol{P}$, $\mathrm{LG}(\boldsymbol{P})$. The exception to this is the case of accidental degeneracies, for which the definition also contains $\boldsymbol{v}$ that are not related by such a transformation. Instructive examples of $\boldsymbol{S}_{\mathfrak{n}}$ are collected in table 2.

Finally, to give the leading-order energy shift, one must make a specific choice for the expansion of $p^\star \cot \delta_0(p^\star)$. For example, if the power-counting is such that

$$p^\star \cot \delta_0(p^\star) = -\frac{1}{a_0} + \mathcal{O}\left(\epsilon^0\right)\,, \tag{2.16}$$

formally holds at all $p^\star$, then the next order is solved by identifying the $1/\epsilon$ term within $f(q_{\mathfrak{n}}, \boldsymbol{d}, L)$

$$f(q_{\mathfrak{n}}, \boldsymbol{d}, L) = -\frac{1}{\epsilon \Delta^{(1)}_{q[\mathfrak{n}]}(L)} \frac{1}{\gamma^{(0)}_{\mathfrak{n}}} \frac{1}{\pi L} \sum_{\boldsymbol{v} \in \boldsymbol{S}_{\mathfrak{n}}} \frac{1}{1 - \partial_{q^2} \Gamma(\boldsymbol{v}|q, \boldsymbol{d}, L)} \bigg|_{q^{(0)}_{\mathfrak{n}}} + \mathcal{O}\left(\epsilon^0\right)\,. \tag{2.17}$$

One can further show that

$$\partial_{q^2} \Gamma(\boldsymbol{v}|q, \boldsymbol{d}, L) \Big|_{q^{(0)}_{\mathfrak{n}}, \boldsymbol{v} \in \boldsymbol{S}_{\mathfrak{n}}} = \left(\frac{\omega_{\boldsymbol{\nu}_{\mathfrak{n}}} - \omega_{\boldsymbol{d} - \boldsymbol{\nu}_{\mathfrak{n}}}}{\omega_{\boldsymbol{\nu}_{\mathfrak{n}}} + \omega_{\boldsymbol{d} - \boldsymbol{\nu}_{\mathfrak{n}}}} \right)^2\,, \tag{2.18}$$

JHEP09(2022)232

where we have introduced

$$\omega_{\boldsymbol{\nu}_\mathfrak{n}} = \sqrt{m^2 + (2\pi/L)^2 \boldsymbol{\nu}_\mathfrak{n}^2}\,, \qquad \omega_{\boldsymbol{d}-\boldsymbol{\nu}_\mathfrak{n}} = \sqrt{m^2 + (2\pi/L)^2\,(\boldsymbol{d}-\boldsymbol{\nu}_\mathfrak{n})^2}\,. \tag{2.19}$$

Simplifying eq. (2.17) and using also that $\Gamma(\boldsymbol{v}|q,\boldsymbol{d},L)$ is the same for all elements of $\boldsymbol{S}_\mathfrak{n}$, we reach

$$\Delta^{(1)}_{q[\mathfrak{n}]}(L) = a_0 \frac{1}{\gamma^{(0)}_\mathfrak{n}} \frac{1}{\pi L} \frac{g_\mathfrak{n} E^{(0)}_\mathfrak{n}(L)^2}{4\omega_{\boldsymbol{\nu}_\mathfrak{n}}\omega_{\boldsymbol{d}-\boldsymbol{\nu}_\mathfrak{n}}}\,. \tag{2.20}$$

Here we have taken $\gamma^{(0)}_\mathfrak{n}$ to denote the boost factor evaluated at the $\mathfrak{n}$th non-interacting energy and have introduced $g_\mathfrak{n}$ as the number of elements within $\boldsymbol{S}_\mathfrak{n}$ ($g_\mathfrak{n} = |\boldsymbol{S}_\mathfrak{n}|$). The corresponding energy can then be written

$$E_\mathfrak{n}(L) = E^{(0)}_\mathfrak{n}(L) + g_\mathfrak{n} \frac{E^{(0)}_\mathfrak{n}(L)}{4\omega_{\boldsymbol{\nu}_\mathfrak{n}}\omega_{\boldsymbol{d}-\boldsymbol{\nu}_\mathfrak{n}}} \frac{8\pi a_0}{\gamma^{(0)}_\mathfrak{n} L^3} + \mathcal{O}\left(\epsilon^2\right)\,. \tag{2.21}$$

This is the main result of this subsection. The appearance of $4\omega_{\boldsymbol{\nu}_\mathfrak{n}}\omega_{\boldsymbol{d}-\boldsymbol{\nu}_\mathfrak{n}}$ can be understood as a relative normalization factor, arising from the definition of the scattering amplitude in terms of relativistically normalized states. The factor $g_\mathfrak{n}$, which can also be traced to normalization of states, implies that higher-multiplicity finite-volume energies may offer more sensitivity to scattering information, at least for weakly interacting systems. Finally, note that the boost factor multiplies the L^3 factor, so that the moving state effectively sees a larger box. This can be roughly interpreted by identifying the L^3 periodicity as the geometry resulting after a length contraction such that the underlying rest-frame volume is effectively larger. We stress again that this result only applies for states that are not accidentally degenerate, i.e. for states in which all elements of $\boldsymbol{S}_\mathfrak{n}$ are related by transformations of the octahedral group or the relevant moving-frame little group, $\mathrm{LG}(\boldsymbol{P})$.

2.3 *S*-wave dominance: all orders

The approach of the previous subsection can now be readily be generalized to all orders. For the left-hand side of eq. (2.9) one substitutes

$$p^\star \cot\delta_0(p^\star) = \sum_{m=0}^{\infty} \frac{1}{m!} \mathcal{K}_m \left(\frac{2\pi}{L}\right)^{2m} \left[q^2 - q^{(0)}_\mathfrak{n}(L)^2\right]^m\,, \tag{2.22}$$

$$= \sum_{m=0}^{\infty} \frac{1}{m!} \mathcal{K}_m \left(\frac{2\pi}{L}\right)^{2m} \left[\sum_{k=1}^{\infty} \epsilon^k\, \Delta^{(k)}_{q[\mathfrak{n}]}(L)\right]^m\,, \tag{2.23}$$

where we have introduced the coefficients

$$\mathcal{K}_m \equiv \left(\frac{\partial}{\partial p^{\star 2}}\right)^m p^\star \cot\delta_0(p^\star)\Big|_{p^{\star 2} = [E^{(0)2}_\mathfrak{n} - \boldsymbol{P}^2]/4 - m^2}\,. \tag{2.24}$$

This is then matched to the expansion of $f(q_\mathfrak{n},\boldsymbol{d},L)$. To give the latter, we first write $f(q_\mathfrak{n},\boldsymbol{d},L)$ in terms of γ and two additional functions

$$f(q_\mathfrak{n},\boldsymbol{d},L) \equiv \frac{1}{\pi L} \frac{\tau_\mathfrak{n}(q_\mathfrak{n},\boldsymbol{d},L) + \beta_\mathfrak{n}(q_\mathfrak{n},\boldsymbol{d},L)}{\gamma(q_\mathfrak{n},\boldsymbol{d},L)}\,, \tag{2.25}$$

JHEP09(2022)232

where

$$\tau_{\mathfrak{n}}(q,\boldsymbol{d},L) \equiv -\sum_{\boldsymbol{v}\in\boldsymbol{S}_{\mathfrak{n}}}\Big[q^2-\Gamma(\boldsymbol{v}|q,\boldsymbol{d},L)\Big]^{-1}, \tag{2.26}$$

$$\beta_{\mathfrak{n}}(q,\boldsymbol{d},L) \equiv -\lim_{s\to -1}\sum_{\boldsymbol{v}\notin\boldsymbol{S}_{\mathfrak{n}}}\Big[q^2-\Gamma(\boldsymbol{v}|q,\boldsymbol{d},L)\Big]^{s}. \tag{2.27}$$

Each of these are then expanded in powers of $q_{\mathfrak{n}}^2(L)-q_{\mathfrak{n}}^{(0)}(L)^2$. For example, we introduce the coefficients $G_{\mathfrak{n},m}$ and $B_{\mathfrak{n},m}$ via

$$\frac{1}{\gamma(q_{\mathfrak{n}},\boldsymbol{d},L)} = \sum_{m=0}^{\infty}\frac{1}{m!}G_{\mathfrak{n},m}(\boldsymbol{d},L)\left[\sum_{k=1}^{\infty}\epsilon^k\,\Delta^{(k)}_{q[\mathfrak{n}]}(L)\right]^m, \tag{2.28}$$

$$\beta_{\mathfrak{n}}(q,\boldsymbol{d},L) = \sum_{m=0}^{\infty}\frac{1}{m!}B_{\mathfrak{n},m}(\boldsymbol{d},L)\left[\sum_{k=1}^{\infty}\epsilon^k\,\Delta^{(k)}_{q[\mathfrak{n}]}(L)\right]^m. \tag{2.29}$$

The τ function, by contrast, starts with a term proportional to the inverse energy shift and can be written as

$$\tau_{\mathfrak{n}}(q_{\mathfrak{n}},\boldsymbol{d},L) = T_{\mathfrak{n},-1}(\boldsymbol{d},L)\left[\sum_{k=1}^{\infty}\epsilon^k\,\Delta^{(k)}_{q[\mathfrak{n}]}(L)\right]^{-1} + \sum_{m=0}^{\infty}\frac{1}{m!}T_{\mathfrak{n},m}(\boldsymbol{d},L)\left[\sum_{k=1}^{\infty}\epsilon^k\,\Delta^{(k)}_{q[\mathfrak{n}]}(L)\right]^m, \tag{2.30}$$

where the above analysis establishes

$$T_{\mathfrak{n},-1}(\boldsymbol{d},L) = -\frac{g_{\mathfrak{n}}E_{\mathfrak{n}}^{(0)}(L)^2}{4\omega_{\boldsymbol{\nu}_{\mathfrak{n}}}\omega_{\boldsymbol{d}-\boldsymbol{\nu}_{\mathfrak{n}}}}. \tag{2.31}$$

The definitions for $G_{\mathfrak{n},m}$, $B_{\mathfrak{n},m}$ and $T_{\mathfrak{n},m}$ can be read off from matching the definitions of the underlying functions and the expansions. The least trivial of these is $T_{\mathfrak{n},m}$ which can be defined as

$$T_{\mathfrak{n},m}(\boldsymbol{d},L) \equiv \left(\frac{\partial}{\partial q^2}\right)^m\left[\frac{g_{\mathfrak{n}}E_{\mathfrak{n}}^{(0)}(L)^2}{4\omega_{\boldsymbol{\nu}_{\mathfrak{n}}}\omega_{\boldsymbol{d}-\boldsymbol{\nu}_{\mathfrak{n}}}}\Big[q^2-q_{\mathfrak{n}}^{(0)}(L)^2\Big]^{-1} - \sum_{\boldsymbol{v}\in\boldsymbol{S}_{\mathfrak{n}}}\Big[q^2-\Gamma(\boldsymbol{v}|q,\boldsymbol{d},L)\Big]^{-1}\right]. \tag{2.32}$$

This collective set of expansions, in particular eqs. (2.28), (2.29) and (2.30), define the main result of this subsection. This completes the discussion of the general strategy for deriving the expansion about non-interacting energies, for both zero and non-zero momenta in the finite-volume frame as well as for all excited states, in the S-wave only truncation. However, to make such an expansion well-defined, one requires an ansatz for $p^\star\cot\delta_0(p^\star)$ as well as a power-counting scheme, as we discuss in the following section.

2.4 Power-counting schemes

In the expansion of the finite-volume energy, eq. (2.7), the ϵ parameter used to organize the expansion is ambiguous. For the rest-frame ground-state energy, $1/L$ serves as a natural parameter and, after working out the details of the expansion, one identifies a_0/L as the relevant dimensionless quantity to identify with ϵ.

JHEP09(2022)232

However, for excited states and for both the ground and excited states in moving frames, it is not always most useful to expand in powers of $1/L$. This is because the non-interacting energy $E_{\mathfrak{n}}^{(0)}(L)$, defined in eq. (2.8) above, is L-dependent. Of course one can simply expand the difference $E_{\mathfrak{n}}(L) - E_{\mathfrak{n}}^{(0)}(L)$ in powers of $1/L$, but as we have shown in eq. (2.21), $E_{\mathfrak{n}}^{(0)}(L)$ also appears as a natural building block at higher orders and expanding this dependence in powers of $1/L$ significantly reduces the descriptive power of the expansion without really simplifying the result.

Based on these considerations, we have found it most useful to organize the expansion by assigning a power-counting scheme to the parameters entering the scattering amplitude, $\mathcal{M}_\ell$. To this end we first give a generalization of the threshold expansion of eq. (2.5). For the ℓ^{th} partial wave one can write

$$p^\star \cot \delta_\ell(p^\star) = -\frac{1}{a_\ell}\left(\frac{1}{p^\star}\right)^{2\ell}\left[1 - \frac{r_\ell a_\ell}{2}p^{\star 2} + O\left(p^{\star 4}\right)\right] . \tag{2.33}$$

Note that, in this convention, the scattering length and the effective range have dimensions that depend on the partial wave of interest, namely

$$[a_\ell] = [E]^{-2\ell-1} \qquad [r_\ell] = [E]^{2\ell-1} . \tag{2.34}$$

It is also possible to expand $p^\star \cot \delta_\ell(p^\star)$ around different values of $p^\star$, not just about threshold.

As a first example we define a *threshold scheme* via

$$a_\ell = \mathcal{O}\left(\epsilon^{2\ell+1}\right) , \qquad a_\ell^2 r_\ell = \mathcal{O}\left(\epsilon^{2\ell+3}\right) , \tag{2.35}$$

with higher orders dictated by assigning $\epsilon^{2\ell+1+n}$ to the $(p^\star)^n$ coefficient in the effective range expansion of $\tan\delta_\ell(p^\star)/p^\star$. This scheme is useful when the contributions from higher-partial waves are suppressed. For example for identical particles with $\boldsymbol{P} = [000]$ and $\Lambda = A_{1g}$, the lowest-lying partial wave contamination arise from $\ell = 4$ and thus appears in this counting at $\mathcal{O}(\epsilon^9)$, corresponding to the $1/L^9$ scaling identified in ref. [11].

An alternative approach is to expand $p^\star \cot \delta_\ell(p^\star)$ about the value of the non-interacting energy. This approach, referred to below as the *weakly-interacting scheme* directly corresponds to eq. (2.23) above. Extending this to all partial waves, we write

$$\mathcal{A}_m^\ell = \mathcal{O}(\epsilon^m) , \tag{2.36}$$

where

$$\mathcal{A}_m^\ell \equiv \left(\frac{\partial}{\partial p^{\star 2}}\right)^m \frac{\tan\delta_\ell(p^\star)}{p^\star}\bigg|_{p^{\star 2}=(2\pi/L)^2 q_{\mathfrak{n}}^{(0)}(L)^2} . \tag{2.37}$$

In contrast to the threshold scheme, the weakly-interacting scheme does not assume suppression of higher partial waves. This power-counting is appropriate, for example, if we are expanding a highly excited state for which $(2\pi/L)^2 q_{\mathfrak{n}}^{(0)}(L)^2$ is order one. As we discuss in the following section, in this regime all partial waves contribute at leading order. Independent of counting $\mathcal{A}_0^\ell$ as leading-order, one must specify the value of this quantity

JHEP09(2022)232

n	$B_{\mathfrak{n},0}$
0	8.9136
1	1.2100
2	5.0961
3	6.7745
4	−9.5381
5	−7.0197
6	23.201

Table 3. Evaluation of the coefficient $B_{\mathfrak{n},0}$ for the first few excited states with $\boldsymbol{P} = [000]$.

to give numerical results. Here it may be useful to re-expand $\tan\delta_\ell(p^\star)$ about threshold, to identify

$$\mathcal{A}_0^\ell = -a_\ell \left(p_{\mathfrak{n}}^{(0)\star}\right)^{2\ell} + \mathcal{O}\left[(p_{\mathfrak{n}}^{(0)\star})^{2\ell+2}\right], \tag{2.38}$$

where $(p_{\mathfrak{n}}^{(0)\star})^2 = (2\pi/L)^2 q_{\mathfrak{n}}^{(0)}(L)^2$. This is the notation used in the following section, but one can easily make the substitution $-a_\ell(p_{\mathfrak{n}}^{(0)\star})^{2\ell} \to \mathcal{A}_0^\ell$ to describe a more general phase shift.

Working to higher orders adds significant complication in general, both due to the fact that the algebra becomes more involved and also because infinite sums appear in the energy expressions beyond leading order. For example, for $\boldsymbol{P} = [000]$, the next-to-next-to-leading-order (NNLO) energy for any excited state in the threshold scheme, is

$$E_{\mathfrak{n}}(L) \equiv E_{\mathfrak{n}}^{(0)}(L) + \epsilon\, g_{\mathfrak{n}} \frac{8\pi a_0}{E_{\mathfrak{n}}^{(0)}(L) L^3} + \epsilon^2\, g_{\mathfrak{n}} \frac{8a_0^2}{E_{\mathfrak{n}}^{(0)}(L) L^4} \left(B_{\mathfrak{n},0} - \frac{4\pi^2 g_{\mathfrak{n}}}{E_{\mathfrak{n}}^{(0)}(L)^2 L^2} \right) + \mathcal{O}\left(\epsilon^3\right), \tag{2.39}$$

where

$$B_{\mathfrak{n},0} \equiv -\lim_{s\to -1} \sum_{\boldsymbol{v}\notin \boldsymbol{S}_{\mathfrak{n}}} \left[q_{\mathfrak{n}}^{(0)2} - \Gamma(\boldsymbol{v}|q_{\mathfrak{n}}^{(0)}, \boldsymbol{d}, L) \right]^s . \tag{2.40}$$

As with the leading-order expression of eq. (2.21), this result only holds for states that are not accidentally degenerate. Numerical values of $B_{\mathfrak{n},0}$ for $\boldsymbol{P} = [000]$ are given in table 3. In the case of non-zero momentum in the finite-volume frame, this quantity inherits an L dependence. Extending the calculation to moving frames or higher orders in the CoM frame becomes quite cumbersome, but can be readily automated using any computer algebra system. This is the motivation for the Mathematica notebook provided in ref. [52] and described briefly at the end of section 3.

2.5 Higher partial waves: without accidental degeneracies

To go beyond the S-wave-only truncation of sections 2.2 and 2.3, we return to the full quantization condition, summarized by eq. (2.2), and evaluate the determinant for a given set of quantum numbers and for some nonzero value of ℓ_{max}. For example, setting $\boldsymbol{P} = [000]$, $\Lambda = A_{1g}$ and $\ell_{\mathsf{max}} = 4$, one reaches a determinant of a two-dimensional matrix that can be written as

$$\det\left[\begin{pmatrix} p\cot\delta_0(p) & 0 \\ 0 & p\cot\delta_4(p) \end{pmatrix} - \begin{pmatrix} f_{00}(q,L) & f_{40}(q,L) \\ f_{40}(q,L) & f_{44}(q,L) \end{pmatrix} \right] = 0\,, \tag{2.41}$$

JHEP09(2022)232

where $f_{\ell\ell'}$ is given by projecting $F_{\ell m;\ell' m'}$ into the trivial irrep of the octahedral group, taking the real part and rescaling by the factor used to relate $F_{00,00}$ to $f(q, \boldsymbol{d}, L)$ in eq. (2.10). The trivial component here matches that of the S-wave only relation $[f_{00}(q, L) = f(q, \mathbf{0}, L)]$ while the others are described in appendix C. The reduction to a two-dimensional matrix arises from the fact that $f_{\ell\ell'} = 0$ whenever ℓ or ℓ' is equal to 1, 2 or 3. Thus, these entries can be dropped without affecting the resulting determinant.

Exactly as for f_{00}, the additional $f_{\ell\ell'}$ functions can be expanded about $q^2 = q_{\mathfrak{n}}^{(0)}(L)^2$ and the condition of vanishing determinant can be solved order by order for a given power-counting scheme. For the threshold scheme, one has to work to very high order to first see the effect of $\ell = 4$. By contrast, in the weakly-interacting scheme, the leading shift for the first excited state (with $q_{\mathfrak{n}}^{(0)}(L)^2 = 1$) already depends on both partial waves.[1] Evaluating eq. (2.41) and expanding, one reaches

$$\Delta_{E[\mathfrak{n}]}^{(1)} = \frac{48\pi}{E_{\mathfrak{n}}^{(0)}(L)L^3}\left(a_0 + \frac{21}{4}a_4\left(p_{\mathfrak{n}}^{(0)}\right)^8\right), \tag{2.42}$$

where $p_{\mathfrak{n}}^{(0)} \equiv 2\pi q_{\mathfrak{n}}^{(0)}/L = 2\pi/L$.

In fact, in the weakly-interacting power-counting scheme, all higher partial waves should be included at leading order. This converts eq. (2.41) to an infinite-dimensional matrix, which can be studied order by order in the expansion. To see how this works at leading order, note that $f_{\ell\ell'}$ is given by

$$\begin{aligned} f_{\ell\ell'}(q, L) &\equiv -8\pi E\, \mathbb{P}_{A_1g,\ell m}\, \mathbb{P}_{A_1g,\ell' m'}\, \mathrm{Re} \lim_{\alpha\to 0^+}\left[\frac{1}{L^3}\sum_{\boldsymbol{k}} - \int_{\boldsymbol{k}}\right]\frac{\mathcal{Y}_{\ell m}(\boldsymbol{k})\mathcal{Y}^*_{\ell' m'}(\boldsymbol{k})e^{-\alpha(k^2-p^2)}}{(2\omega_{\boldsymbol{k}})^2(E - 2\omega_{\boldsymbol{k}} + i\epsilon)}, \\ &= -\frac{8\pi g_{\mathfrak{n}}}{E_{\mathfrak{n}}^{(0)}(L)L^3}\frac{M^{\mathfrak{n}}_{\ell\ell'}}{\epsilon\Delta_{E[\mathfrak{n}]}^{(1)}} + \mathcal{O}(\epsilon^0), \end{aligned} \tag{2.43}$$

where the definition is taken from appendix A and $\mathcal{Y}_{\ell m}(\boldsymbol{k}) = \sqrt{4\pi}(k/p)^\ell Y_{\ell m}(\hat{\boldsymbol{k}})$. We introduce $\mathbb{P}_{A_1g,\ell m}$, which projects the ℓ^{th} partial wave into the trivial irrep and

$$M^{\mathfrak{n}}_{\ell\ell'} = 4\pi\mathbb{P}_{A_1g,\ell m}\, \mathbb{P}_{A_1g,\ell' m'}\frac{1}{|O_h|}\sum_{R\in O_h} Y_{\ell m}(R\cdot\hat{\boldsymbol{\nu}}_{\mathfrak{n}})Y^*_{\ell' m'}(R\cdot\hat{\boldsymbol{\nu}}_{\mathfrak{n}}). \tag{2.44}$$

As we show in appendix C, this can be rewritten as

$$M^{\mathfrak{n}}_{\ell\ell'} = \sqrt{\mathcal{P}^{\mathfrak{n}}_\ell}\sqrt{\mathcal{P}^{\mathfrak{n}}_{\ell'}}, \tag{2.45}$$

where

$$\mathcal{P}^{\mathfrak{n}}_\ell = (2\ell+1)\frac{1}{|O_h|}\sum_{R\in O_h} P_\ell(\hat{\boldsymbol{\nu}}_{\mathfrak{n}}\cdot R\cdot\hat{\boldsymbol{\nu}}_{\mathfrak{n}}), \tag{2.46}$$

and $P_\ell(\hat{\boldsymbol{\nu}}_{\mathfrak{n}}\cdot R\cdot\hat{\boldsymbol{\nu}}_{\mathfrak{n}}) = P_\ell(\cos\theta)$ is the ℓ^{th} Legendre polynomial. The first few non-zero values of $\mathcal{P}^{\mathfrak{n}}_\ell$ are summarized in table 4. The key point is that $M^{\mathfrak{n}}_{\ell\ell'}$ is a rank-one matrix, which

[1] The effect of higher partial waves on the ground state is suppressed in both schemes. This is because the shift away from threshold, required to induce dependence on δ_ℓ with $\ell > 0$, arises only due to the interactions. Thus the leading higher-partial waves appear in a product with parameters describing the S-wave interaction.

JHEP09(2022)232

$\boldsymbol{P} = [000]$

ℓ	$q_{\mathfrak{n}}^{(0)}(L)^2 = 1$		$q_{\mathfrak{n}}^{(0)}(L)^2 = 2$		$q_{\mathfrak{n}}^{(0)}(L)^2 = 3$	
0	1		1		1	
4	$\frac{21}{4}$	5.25000	$\frac{21}{64}$	0.32813	$\frac{7}{3}$	2.33333
6	$\frac{13}{8}$	1.62500	$\frac{2197}{512}$	4.29102	$\frac{416}{81}$	5.13580
8	$\frac{561}{64}$	8.76563	$\frac{45441}{16384}$	2.77350	$\frac{187}{243}$	0.76955
10	$\frac{455}{128}$	3.55469	$\frac{455}{131072}$	0.00347	$\frac{58240}{6561}$	8.87670
12	$\frac{18575}{1536}$	12.0931	$\frac{56638775}{6291456}$	9.00249	$\frac{763975}{177147}$	4.31266
14	$\frac{17255}{3072}$	5.61686	$\frac{136676855}{50331648}$	2.71553	$\frac{1104320}{177147}$	6.23392
16	$\frac{251009}{16384}$	15.3204	$\frac{3525395489}{1073741824}$	3.28328	$\frac{6464161}{531441}$	12.1635
18	$\frac{254227}{32768}$	7.75839	$\frac{83891347603}{8589934592}$	9.76624	$\frac{170017664}{43046721}$	3.94961
20	$\frac{2422567}{131072}$	18.4827	$\frac{922978270207}{137438953472}$	6.71555	$\frac{1881436823}{129140163}$	14.5690

Table 4. Numerical values for the $\mathcal{P}_\ell^{\mathfrak{n}}$ coefficients, giving the contribution of the ℓ^{th} partial wave to the first few excited states with $\Lambda = A_{1g}$ and $\boldsymbol{P} = [000]$.

allows one to analytically evaluate the leading-order determinant. Note that this is only valid when one is expanding about a state that does not exhibit accidental degeneracy. The latter case is discussed in detail in the following subsection.

Combining eqs. (2.2), (2.41), (2.43) and (2.45), we reach a determinant of the form

$$\det\left[\underline{p\cot\delta(p)} + \frac{8\pi g_{\mathfrak{n}}}{E_{\mathfrak{n}}^{(0)}(L)L^3}\frac{1}{\epsilon\Delta_{E[\mathfrak{n}]}^{(1)}}\sqrt{\mathcal{P}^{\mathfrak{n}}}\otimes\sqrt{\mathcal{P}^{\mathfrak{n}}}\right] = 0\,, \tag{2.47}$$

where $\otimes$ indicates an outer product of the two vectors and $\underline{p\cot\delta(p)}$ is a diagonal matrix populated by $p\cot\delta_\ell(p)$. This can be rewritten as the eigenvalue equation

$$\left[1 + \frac{8\pi g_{\mathfrak{n}}}{E_{\mathfrak{n}}^{(0)}(L)L^3}\frac{1}{\epsilon\Delta_{E[\mathfrak{n}]}^{(1)}}\sqrt{\frac{\tan\delta(p)}{p}}\sqrt{\mathcal{P}^{\mathfrak{n}}}\otimes\sqrt{\mathcal{P}^{\mathfrak{n}}}\sqrt{\frac{\tan\delta(p)}{p}}\right]\boldsymbol{\mathcal{E}} = 0\,. \tag{2.48}$$

Guessing a solution of the form $\boldsymbol{\mathcal{E}} = \sqrt{\frac{\tan\delta(p)}{p}}\sqrt{\mathcal{P}^{\mathfrak{n}}}$ then yields

$$0 = \left[1 + \frac{8\pi g_{\mathfrak{n}}}{E_{\mathfrak{n}}^{(0)}(L)L^3}\frac{1}{\epsilon\Delta_{E[\mathfrak{n}]}^{(1)}}\sqrt{\frac{\tan\delta(p)}{p}}\sqrt{\mathcal{P}^{\mathfrak{n}}}\otimes\sqrt{\mathcal{P}^{\mathfrak{n}}}\sqrt{\frac{\tan\delta(p)}{p}}\right]\cdot\sqrt{\frac{\tan\delta(p)}{p}}\sqrt{\mathcal{P}^{\mathfrak{n}}}\,, \tag{2.49}$$

$$= \left[1 + \frac{8\pi g_{\mathfrak{n}}}{E_{\mathfrak{n}}^{(0)}(L)L^3}\frac{1}{\epsilon\Delta_{E[\mathfrak{n}]}^{(1)}}\left(\sqrt{\mathcal{P}^{\mathfrak{n}}}\cdot\frac{\tan\delta(p)}{p}\cdot\sqrt{\mathcal{P}^{\mathfrak{n}}}\right)\right]\boldsymbol{\mathcal{E}}\,, \tag{2.50}$$

where we stress that $\sqrt{\tan\delta(p)/p}$ is a diagonal matrix and $\sqrt{\mathcal{P}^{\mathfrak{n}}}$ and $\boldsymbol{\mathcal{E}}$ are column vectors. The square bracketed quantity is thus a scalar quantity and it remains to enforce the

JHEP09(2022)232

vanishing of this combination

$$1 + \frac{8\pi g_{\mathfrak{n}}}{E_{\mathfrak{n}}^{(0)}(L)L^3} \frac{1}{\epsilon \Delta_{E[\mathfrak{n}]}^{(1)}} \left(\sqrt{\mathcal{P}^{\mathfrak{n}}} \cdot \frac{\tan\delta(p)}{p} \cdot \sqrt{\mathcal{P}^{\mathfrak{n}}} \right) = 0 \,. \tag{2.51}$$

Substituting the leading-order relation $p \cot \delta_\ell(p) = -\left[a_\ell (p_{\mathfrak{n}}^{(0)})^{2\ell}\right]^{-1}$ and solving for the energy shift, one finally reaches

$$\Delta_{E[\mathfrak{n}]}^{(1)} = \frac{8\pi g_{\mathfrak{n}}}{E_{\mathfrak{n}}^{(0)}(L)L^3} \sum_{\ell=0}^{\infty} \mathcal{P}_\ell^{\mathfrak{n}} \, a_\ell \left(p_{\mathfrak{n}}^{(0)}\right)^{2\ell} . \tag{2.52}$$

A similar result to this was already derived in ref. [10], with $E_{\mathfrak{n}}^{(0)}(L)$ expanded about $L = \infty$. As mentioned above, this result can be re-expressed using $-a_\ell (p_{\mathfrak{n}}^{(0)})^{2\ell} \to \mathcal{A}_0^\ell$, in case one has a better description of $\tan\delta_\ell(p_{\mathfrak{n}}^{(0)})$ than is given by its leading-order threshold expansion.

This can be readily generalized to non-zero $\boldsymbol{P}$, taking advantage of the fact that $f_{\ell\ell'}(q, \boldsymbol{d}, L)$ is also a rank-one matrix at leading order, when expanded about a non-degenerate state in the moving frame. One finds

$$f_{\ell\ell'}(q, \boldsymbol{d}, L) = -\frac{E_{\mathfrak{n}}^{(0)}(L)}{4\omega_{\boldsymbol{\nu}_{\mathfrak{n}}}\omega_{\boldsymbol{d}-\boldsymbol{\nu}_{\mathfrak{n}}}} \frac{8\pi g_{\mathfrak{n}}}{\gamma_{\mathfrak{n}}^{(0)} L^3} \frac{\sqrt{\mathcal{P}_\ell^{\mathfrak{n}}}\sqrt{\mathcal{P}_{\ell'}^{\mathfrak{n}}}}{\epsilon \Delta_{E[\mathfrak{n}]}^{(1)}} + \mathcal{O}\left(\epsilon^0\right) , \tag{2.53}$$

from which follows

$$\Delta_{E[\mathfrak{n}]}^{(1)} = \frac{E_{\mathfrak{n}}^{(0)}(L)}{4\omega_{\boldsymbol{\nu}_{\mathfrak{n}}}\omega_{\boldsymbol{d}-\boldsymbol{\nu}_{\mathfrak{n}}}} \frac{8\pi g_{\mathfrak{n}}}{\gamma_{\mathfrak{n}}^{(0)} L^3} \sum_{\ell=0}^{\infty} \mathcal{P}_\ell^{\mathfrak{n}} \, a_\ell \left(p_{\mathfrak{n}}^{(0)\star}\right)^{2\ell} , \tag{2.54}$$

where

$$\mathcal{P}_\ell^{\mathfrak{n}} = (2\ell+1) \frac{1}{|\mathrm{LG}(\boldsymbol{P})|} \sum_{R \in \mathrm{LG}(\boldsymbol{P})} P_\ell(\hat{\boldsymbol{\nu}}_{\mathfrak{n}}^\star \cdot R \cdot \hat{\boldsymbol{\nu}}_{\mathfrak{n}}^\star) \,. \tag{2.55}$$

Here $\mathrm{LG}(\boldsymbol{P})$ is the relevant little group for the indicated total momentum, i.e. the subgroup of O_h under which $\boldsymbol{P}$ is left invariant. In general, $\mathcal{P}_\ell^{\mathfrak{n}}$ depends on $\gamma_{\mathfrak{n}}^{(0)}$, the Lorentz boost factor. For example, for $\boldsymbol{P} = [001]$ and $\boldsymbol{\nu}_{\mathfrak{n}} = (0,1,1)$, the lowest lying components are

$$\mathcal{P}_2^{\mathfrak{n}} = \frac{5\left(1-2\gamma^2\right)^2}{\left(1+4\gamma^2\right)^2} , \qquad \mathcal{P}_4^{\mathfrak{n}} = \frac{9\left(1-24\gamma^2+156\gamma^4-144\gamma^6+176\gamma^8\right)}{\left(1+4\gamma^2\right)^4} , \tag{2.56}$$

where we have abbreviated $\gamma = \gamma_{\mathfrak{n}}^{(0)}$. The gamma dependence translates to a dependence on mL at fixed $\mathfrak{n}$ and $\boldsymbol{d}$.

While the numerical values of $\mathcal{P}_\ell^{\mathfrak{n}}$ for a given mL can be easily determined, the expressions in terms of $\gamma_{\mathfrak{n}}^{(0)}$ become very complicated. Therefore, instead of giving additional analytic expressions, we provide numerical values for several states and total momenta at $mL = 4$ and 6. These are collected in tables 5, 6, 7 and 8, which give results for $\boldsymbol{P} = [001]$, [011], [111] and [002] respectively. Cases do arise for which $\boldsymbol{\nu}_{\mathfrak{n}}^\star$ and $\mathcal{P}_\ell^{\mathfrak{n}}$ do not depend on $\gamma_{\mathfrak{n}}^{(0)}$. These include trivial examples, in which $\boldsymbol{\nu}_{\mathfrak{n}}$ is parallel to $\boldsymbol{d}$, as well as more interesting cases in which a cancellation occurs in the definition of the boost. See tables 6 and 8 for detailed examples.

JHEP09(2022)232

$\boldsymbol{P} = [001]$								
	$\boldsymbol{\nu}_\mathfrak{n} = (0,0,0)$		$\boldsymbol{\nu}_\mathfrak{n} = (0,1,1)$		$\boldsymbol{\nu}_\mathfrak{n} = (1,1,1)$		$\boldsymbol{\nu}_\mathfrak{n} = (0,1,2)$	
mL	4	6	4	6	4	6	4	6
$\gamma_\mathfrak{n}^{(0)}$ / ℓ	1.19626	1.10634	1.07431	1.05691	1.04639	1.03900	1.03504	1.03055
0	1		1		1		1	
2	5		0.27129	0.25468	0.59963	0.59284	1.33212	1.34687
4	9		2.45998	2.43769	3.20612	3.18518	0.27682	0.26394
6	13		2.61771	2.77009	0.40378	0.42879	3.66277	3.64266
8	17		5.61785	5.46126	5.77910	5.81357	5.75364	5.75043
10	21		5.34109	5.30821	5.63594	5.67937	6.21060	6.25678
12	25		3.22650	3.27018	7.92711	7.79359	2.73187	2.79102
14	29		11.1664	11.4538	5.60555	5.58544	7.11547	6.90712
16	33		6.01485	5.62644	6.05785	6.07222	13.4850	13.5607
18	37		10.8386	10.6632	10.9403	11.1847	6.22219	6.46048
20	41		6.67668	7.40405	10.7249	10.6259	7.20059	6.96068

Table 5. Numerical values of the $\mathcal{P}_\ell^\mathfrak{n}$ coefficients, giving the leading-order contribution of the ℓ^{th} partial wave to the first few low-lying states for $\Lambda = A_1$ and $\boldsymbol{P} = [001]$. The coefficients generally depend on the Lorentz boost factor $\gamma_\mathfrak{n}^{(0)}$ but with exceptions, such as $\boldsymbol{\nu}_\mathfrak{n} = (0,0,0)$ here. For this special case one simply has $\mathcal{P}_\ell^\mathfrak{n} = (2\ell+1)$. In the general case $\mathcal{P}_\ell^\mathfrak{n}$ depends on mL and here we evaluate the coefficients for $mL = 4$ and $mL = 6$ as indicated.

2.6 Higher partial waves: including accidental degeneracies

We turn now to the case that the non-interacting states, about which we are expanding, are accidentally degenerate. This occurs whenever one can identify two (or more) values of representative momenta $\boldsymbol{\nu}_{\mathfrak{n},1}$ and $\boldsymbol{\nu}_{\mathfrak{n},2}$ such that the corresponding energies are equal for all L,[2] i.e.

$$E_{\mathfrak{n},1}(L) = E_{\mathfrak{n},2}(L)\,, \tag{2.57}$$

for

$$E_{\mathfrak{n},i}(L) \equiv \sqrt{m^2 + (2\pi/L)^2 \boldsymbol{\nu}_{\mathfrak{n},i}^2} + \sqrt{m^2 + (2\pi/L)^2 (\boldsymbol{d} - \boldsymbol{\nu}_{\mathfrak{n},i})^2}\,, \tag{2.58}$$

but with the property that the vectors corresponding to $i = 1$ and $i = 2$ cannot be rotated into one another. In particular, the state is accidentally degenerate provided that no little-group rotation exists $R \in \mathrm{LG}(\boldsymbol{P})$ for which $R \cdot \boldsymbol{\nu}_{\mathfrak{n},1}$ is equal to either $\boldsymbol{\nu}_{\mathfrak{n},2}$ or $\boldsymbol{d} - \boldsymbol{\nu}_{\mathfrak{n},2}$.

[2] Another special case arises when two energies coincide only for a single, finely tuned value of mL. Here the non-degenerate expansion can be performed at any L away from the finely tuned point. One then manifestly sees a breakdown in the form of diverging expansion coefficients as L approaches the crossing. An alternative expansion, performed exactly at the degenerate point and treating the accidental degeneracy as described here would resolve the issue and give the correct avoided-level-crossing behavior.

JHEP09(2022)232

$\boldsymbol{P} = [011]$

	$\boldsymbol{\nu}_\mathfrak{n} = (0,0,0)$		$\boldsymbol{\nu}_\mathfrak{n} = (1,1,1)$		$\boldsymbol{\nu}_\mathfrak{n} = (1,1,0)$		$\boldsymbol{\nu}_\mathfrak{n} = (0,1,2)$	
mL	4	6	4	6	4	6	4	6
ℓ \ $\gamma_\mathfrak{n}^{(0)}$	1.31075	1.18046	1.13063	1.10236	1.12358	1.09877	1.09259	1.07675
0	1		1		1		1	
2	5		1.96835	1.90202	$\frac{5}{3} \sim 1.66667$		2.34477	2.38673
4	9		3.67737	3.84859	$\frac{41}{9} \sim 4.55556$		2.93896	2.88123
6	13		8.60380	8.51008	$\frac{1885}{243} \sim 7.75720$		8.35018	8.25431
8	17		6.65130	6.38607	$\frac{4505}{729} \sim 6.17970$		8.87560	9.13679
10	21		10.3638	11.0137	$\frac{254261}{19683} \sim 12.9178$		7.79505	7.70573
12	25		14.9275	14.3335	$\frac{5956625}{531441} \sim 11.2084$		14.5092	14.1373
14	29		11.4305	11.3172	$\frac{7345903}{531441} \sim 13.8226$		15.8750	16.3929
16	33		17.7535	18.8254	$\frac{30465875}{1594323} \sim 19.1090$		12.9680	13.0249
18	37		20.3293	18.8820	$\frac{1932764005}{129140163} \sim 14.9664$		20.0635	19.2635
20	41		16.7256	17.3828	$\frac{9057620329}{387420489} \sim 23.3793$		23.0663	23.7404

Table 6. As in table 5 but for $\boldsymbol{P} = [011]$. Note that here two cases arise for which $\mathcal{P}_\ell^\mathfrak{n}$ is independent of mL, the trivial case with $\boldsymbol{\nu}_\mathfrak{n} = (0,0,0)$ and a more interesting case with $\boldsymbol{\nu}_\mathfrak{n} = (1,1,0)$.

$\boldsymbol{P} = [111]$

	$\boldsymbol{\nu}_\mathfrak{n} = (0,0,0)$		$\boldsymbol{\nu}_\mathfrak{n} = (0,0,1)$		$\boldsymbol{\nu}_\mathfrak{n} = (0,0,-1)$		$\boldsymbol{\nu}_\mathfrak{n} = (0,1,2)$	
mL	4	6	4	6	4	6	4	6
ℓ \ $\gamma_\mathfrak{n}^{(0)}$	1.39618	1.23919	1.29171	1.20769	1.13026	1.10865	1.11783	1.10111
0	1		1		1		1	
2	5		0.78193	0.72807	1.59464	1.66216	0.11819	0.10608
4	9		2.37330	2.53029	0.74414	0.67119	0.59680	0.64024
6	13		6.82511	6.67527	6.46793	6.27289	2.63788	2.57512
8	17		2.59823	2.50325	6.98998	7.37341	4.73931	4.78323
10	21		8.52575	9.01303	3.20973	3.24944	1.19544	1.13906
12	25		9.76633	9.05537	9.73565	9.01811	3.28963	3.49965
14	29		5.74940	6.19649	13.0258	13.5804	8.75731	8.34118
16	33		15.1005	15.4210	6.78710	7.40763	2.39753	2.75679
18	37		10.7882	9.61485	11.7747	10.4662	6.48135	6.55101
20	41		11.3319	12.7961	18.7898	18.9909	6.61792	6.18188

Table 7. As in table 5 but for $\boldsymbol{P} = [111]$.

JHEP09(2022)232

$\boldsymbol{P} = [002]$

	$\boldsymbol{\nu}_\mathfrak{n} = (0,0,0)$		$\boldsymbol{\nu}_\mathfrak{n} = (0,1,1)$		$\boldsymbol{\nu}_\mathfrak{n} = (1,1,2)$		$\boldsymbol{\nu}_\mathfrak{n} = (0,1,2)$	
mL	4	6	4	6	4	6	4	6
ℓ \ $\gamma_\mathfrak{n}^{(0)}$	1.46576	1.28858	1.30828	1.23412	1.14714	1.12709	1.21680	1.17441
0	1		1		1		1	
2	5		$\frac{5}{4} \sim 1.25$		0.03784	0.02915	0.05480	0.08510
4	9		$\frac{99}{16} \sim 6.18750$		2.31286	2.31576	2.25597	2.20657
6	13		$\frac{143}{32} \sim 4.46875$		4.82646	4.90205	4.87130	4.76372
8	17		$\frac{2771}{256} \sim 10.8242$		1.70987	1.49774	1.90006	2.41449
10	21		$\frac{4053}{512} \sim 7.91602$		7.57424	7.83763	6.77813	5.80645
12	25		$\frac{31375}{2048} \sim 15.3198$		4.88759	4.82769	6.52095	7.59568
14	29		$\frac{46951}{4096} \sim 11.4626$		7.73567	7.34108	5.64314	5.10550
16	33		$\frac{1293699}{65536} \sim 19.7403$		8.16988	8.99679	9.47708	8.99164
18	37		$\frac{1975097}{131072} \sim 15.0688$		8.99199	8.14196	10.1730	11.5729
20	41		$\frac{12641653}{524288} \sim 24.1120$		11.4709	11.7618	6.75650	5.17772

Table 8. As in table 5 but for $\boldsymbol{P} = [002]$. As with table 6 a non-trivial case of mL independence arises.

Equivalently, the $\mathfrak{n}$ state is accidentally degenerate whenever the elements of the set $\boldsymbol{S}_\mathfrak{n}$, defined in eq. (2.15), are not related by rotations within the little group.

The standard example is the state with $q_\mathfrak{n}^{(0)}(L)^2 = 9$ and $\boldsymbol{P} = [000]$, which includes $\boldsymbol{\nu}_{\mathfrak{n},1} = (1,2,2)$ and $\boldsymbol{\nu}_{\mathfrak{n},2} = (0,0,3)$. In this case, the set $\boldsymbol{S}_\mathfrak{n}$ naturally decomposes into two subsets, given by all rotations of the two momentum types, and we say the state is two-fold degenerate. The degeneracy is broken by the lowest non-vanishing angular momentum that couples to the system, $\ell = 4$. Setting $\ell_{\mathsf{max}} = 4$ and expanding $f_{\ell\ell'}$ to leading order gives

$$\begin{pmatrix} f_{00}(q,L) & f_{40}(q,L) \\ f_{40}(q,L) & f_{44}(q,L) \end{pmatrix} = -\frac{240\pi}{E_\mathfrak{n}^{(0)}(L)L^3}\frac{1}{\epsilon\Delta_{E[\mathfrak{n}]}^{(1)}}\begin{pmatrix} 1 & \frac{5}{18}\sqrt{\frac{7}{3}} \\ \frac{5}{18}\sqrt{\frac{7}{3}} & \frac{1967}{972} \end{pmatrix} + \mathcal{O}\left(\epsilon^0\right), \tag{2.59}$$

where crucially, and in contrast to the case analyzed in the previous subsection, the leading-order part of $f_{\ell\ell'}$ is no longer rank one and thus multiple solutions arise. Substituting into eq. (2.41), expanding to leading order in $a_0, a_4 = \mathcal{O}(\epsilon)$ and solving for the leading-order energy shift, one finds

$$\Delta_{E[\mathfrak{n}],\pm}^{(1)}(L) = \frac{120\pi}{E_\mathfrak{n}^{(0)}(L)L^3}\left(\alpha \pm \sqrt{\beta}\right), \tag{2.60}$$

$$\alpha = a_0 + \frac{1967}{972}a_4\left(p_\mathfrak{n}^{(0)}\right)^8, \tag{2.61}$$

$$\beta = a_0^2 - \frac{539}{162}a_0a_4\left(p_\mathfrak{n}^{(0)}\right)^8 + \left(\frac{1967}{972}\right)^2 a_4^2\left(p_\mathfrak{n}^{(0)}\right)^{16}. \tag{2.62}$$

JHEP09(2022)232

Expanding the split states about $a_4 = 0$ then yields

$$\Delta^{(1)}_{E[\mathfrak{n}],+}(L) = \frac{240\pi}{E^{(0)}_{\mathfrak{n}}(L)L^3} a_0 + \mathcal{O}(a_4)\,, \tag{2.63}$$

$$\Delta^{(1)}_{E[\mathfrak{n}],-}(L) = \frac{35840\pi}{81E^{(0)}_{\mathfrak{n}}(L)L^3} a_4 \left(p^{(0)}_{\mathfrak{n}}\right)^8 + \mathcal{O}\left(a_4^2\right)\,. \tag{2.64}$$

It is interesting to note that $\Delta^{(1)}_{E[\mathfrak{n}],+}(L)$ matches the naive non-degenerate result of eq. (2.21) with $g_{\mathfrak{n}} = 30$ counting rotations and flips of both $(1,2,2)$ and $(0,0,3)$ within $S_{\mathfrak{n}}$. (See also table 2.)

A similar calculation can be used to deduce the leading splitting for any accidentally generate state with any value of $\boldsymbol{P}$. Odd partial waves never contribute, since $\delta_\ell(p) = 0$ for identical particles with odd ℓ. However, in the case of non-zero total momentum, the projected geometric function $f_{\ell\ell'}$ is nonzero for $\ell, \ell' = 2$ and $\delta_2(p)$ does enter the energy shift. As with the example presented above, the leading-order energies can always be determined by identifying the value of ℓ_{max} required to break the accidental degeneracy and solving the quantization condition truncated to this order.

Rather than give a large number of examples, here we summarize two key observations, proven in appendix E:

- For non-zero $\boldsymbol{P}$, the accidental degeneracy is sometimes broken only by $\ell = 4$, even when $\ell = 2$ contributes to the energy shifts. In particular, one can show that for all states with $\boldsymbol{P} = [00a]$ and $\boldsymbol{P} = [aaa]$, $\ell_{\mathsf{max}} = 4$ is required to split degenerate levels. For all other momentum types, the splitting occurs with $\ell_{\mathsf{max}} = 2$.

- Determining the leading shift in a power-counting for which a finite set of partial waves are counted as the same order, $a_\ell = \mathcal{O}(\epsilon)$, one generically recovers expressions like eq. (2.60), i.e. not polynomials in the partial-wave coefficients. However, expanding the resulting solutions about $a_\ell = 0$ for all non-zero ℓ, one always recovers one shift of the form

  $$\Delta^{(1)}_{E[\mathfrak{n}],+}(L) = g_{\mathfrak{n}} \frac{E^{(0)}_{\mathfrak{n}}(L)}{4\omega_{\boldsymbol{\nu}_{\mathfrak{n}}}\omega_{\boldsymbol{d}-\boldsymbol{\nu}_{\mathfrak{n}}}} \frac{8\pi a_0}{\gamma^{(0)}_{\mathfrak{n}} L^3}\,. \tag{2.65}$$

  This is the naive result for non-degenerate states given in eq. (2.60). In the case of a two-fold degeneracy, the other state has a shift of the form

  $$\Delta^{(1)}_{E[\mathfrak{n}],-}(L) \propto a_{\ell_B} \left(p^{(0)}_{\mathfrak{n}}\right)^{2\ell_B}\,, \tag{2.66}$$

  where ℓ_B is the lowest partial wave that is required to split the degeneracy.

3 Numerical checks

In the previous section we have laid out a systematic method for expanding a given finite-volume energy in an arbitrary frame to any desired order in a specified power-counting scheme. We have additionally presented the explicit leading-order, and in certain cases higher-order, energy shifts for any non-degenerate state.

The specific results given depend on details of the state and the scheme used. In the threshold scheme, in which the S-wave dominates, we give the NLO expression for general

JHEP09(2022)232

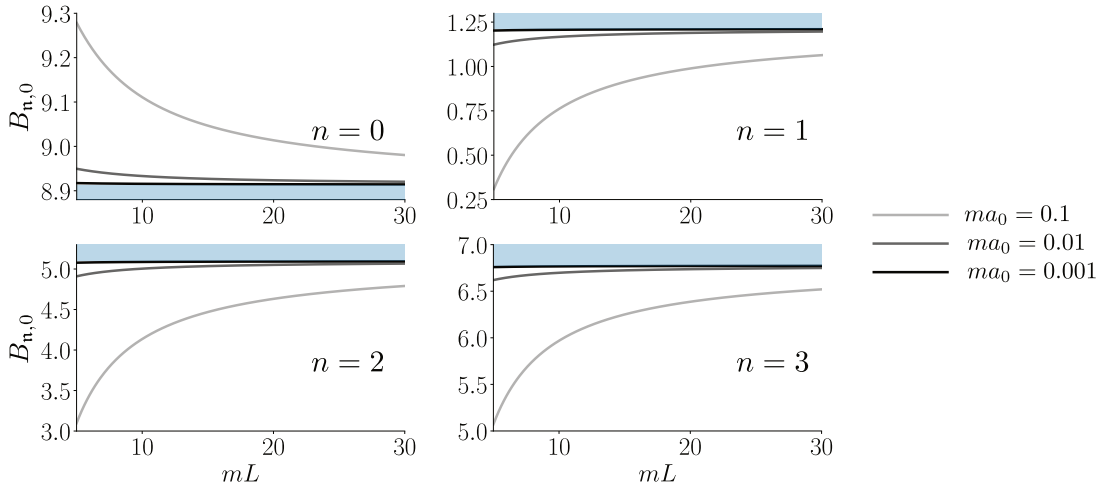

Figure 1. Result of equating the numerically determined finite-volume energy, $E_{\mathfrak{n}}(L)$, to the truncated expansion of eq. (2.39) and solving for the leading coefficient, $B_{\mathfrak{n},0}$. The extraction is performed for the ground state ($n = 0$) and the first three excited states ($n = 1, 2, 3$) all for $\boldsymbol{P} = [000]$ and for three different values of ma_0, as indicated in the legend. The border between the shaded blue and the unshaded regions indicates the numerical value of $B_{\mathfrak{n},0}$ in each case, given by explicitly evaluating the sum defined in eq. (2.40). As expected, the extraction from the full $E_{\mathfrak{n}}(L)$ value approaches the expected value as mL increases and, for fixed mL, also as ma_0 decreases.

momentum $\boldsymbol{P}$ and general excitation n in eq. (2.21) and the NNLO expression for $\boldsymbol{P} = [000]$ in eq. (2.39). The result in the weakly-interacting scheme is given in eq. (2.54) and contains an infinite sum over angular momentum components with known coefficients. (See also tables 4–8.) Finally, section 2.6 summarizes the leading-order results in the case of an accidentally degenerate state. Here the expansion must be performed, at least initially, treating the degeneracy-breaking partial wave as leading order.

In this section we summarize two tests that verify our methods and provide a cross check on the expressions presented in this work. Both make use of the fact that one can numerically solve the S-wave quantization condition for weakly interacting systems and numerically compare to the expanded result.

The first check explicitly addresses eq. (2.39) by taking this result, truncated to the order written, then substituting in the numerical determination of $E_{\mathfrak{n}}(L)$ and finally solving for an effective $B_{\mathfrak{n},0}$

$$B_{\mathfrak{n},0}^{\mathsf{eff}}(L) \equiv \left[E_{\mathfrak{n}}(L) - E_{\mathfrak{n}}^{(0)}(L) - g_{\mathfrak{n}} \frac{8\pi a_0}{E_{\mathfrak{n}}^{(0)}(L) L^3}\right] \left(g_{\mathfrak{n}} \frac{8a_0^2}{E_{\mathfrak{n}}^{(0)}(L) L^4}\right)^{-1} + \frac{4\pi^2 g_{\mathfrak{n}}}{E_{\mathfrak{n}}^{(0)}(L)^2 L^2}\,. \tag{3.1}$$

As we confirm in figure 1, this quantity asymptotes to the values listed in table 3. The approach to the plateau is consistent with the expected scaling

$$B_{\mathfrak{n},0}^{\mathsf{eff}}(L) = B_{\mathfrak{n},0} + \mathcal{O}(a_0/L)\,. \tag{3.2}$$

The second check addresses eq. (2.21) and shows that the difference between our analytic expression and the numerical result from the quantization condition decreases in magnitude

JHEP09(2022)232

as one goes to higher orders in the expansion. This check is performed by subtracting first the LO term (the non-interacting energy) followed by the next-to-leading-order (NLO) correction (the correction proportional to a_0). We carry out this analysis for three values of total momenta — $\boldsymbol{P} = [000], [001], [011]$ — and for the four lowest states in each frame. The results of this comparison are shown in figure 2.

As mentioned above, we have also provided a Mathematica [51] notebook via ref. [52], that automates the systematic expansion of finite-volume energies assuming S-wave interactions in the trivial irrep, as detailed in section 2. This allows one to specify any type of interaction, via the two-particle scattering phase shift, and to pass any type of power-counting scheme to define the expansion order by order. The user can additionally specify a total momentum and representative momentum in order to indicate the non-interacting excited state about which the expansion is performed, as well as the order of the expansion. Further options are available to adjust which of the building blocks entering the expansion are left implicit. We include several descriptive examples within the notebook itself and so will not give further details here.

4 Conclusion and outlook

In this work we have presented analytic expansions of finite-volume two-particle excited states for any value of spatial momentum, $\boldsymbol{P}$, defined with respect to the finite-volume frame. The results were derived using Lüscher's finite-volume scattering formalism and its extension to the moving frame, and provide intuition for numerical solutions of the latter. In contrast to the rest-frame ground state, for non-zero $\boldsymbol{P}$ and for excited states, the inverse box length $1/L$ no longer neccesarily defines a useful expansion parameter. This is because the non-interacting energy and the Lorentz boost factor both depend on the volume, and expanding these, as they appear within the energy shift, degrades the range of validity without really simplifying the results. The preferred method is thus to parametrize the scattering amplitude, and to assign a power-counting scheme to the relevant parameters in order to organize the series. This is discussed in section 2.4.

The general method and concrete results, detailed in section 2, apply to a single channel of identical spinless particles. Attention is also restricted to finite-volume energies in the trivial irrep of the symmetry group, but we do include the effects of higher orbital angular momenta, which contribute to the trivial irrep due to the reduced rotational symmetry of the cubic box. As is discussed in detail in section 2.6, non-trivial partial waves play a particularly interesting role in the case of accidentally degenerate states, for which they are required to split the degeneracy.

The main motivation of this work is to establish the method, and the necessary inputs, for an analogous expansion of three-particle finite-volume excited states with generic $\boldsymbol{P}$. We have derived these results in parallel, by expanding the three-particle quantization condition of refs. [24, 25]. The results will be presented in a separate manuscript. The expressions for three-particle states are expected to be particularly useful since the full numerical machinery is significantly more complicated than in the two-particle sector.

JHEP09(2022)232

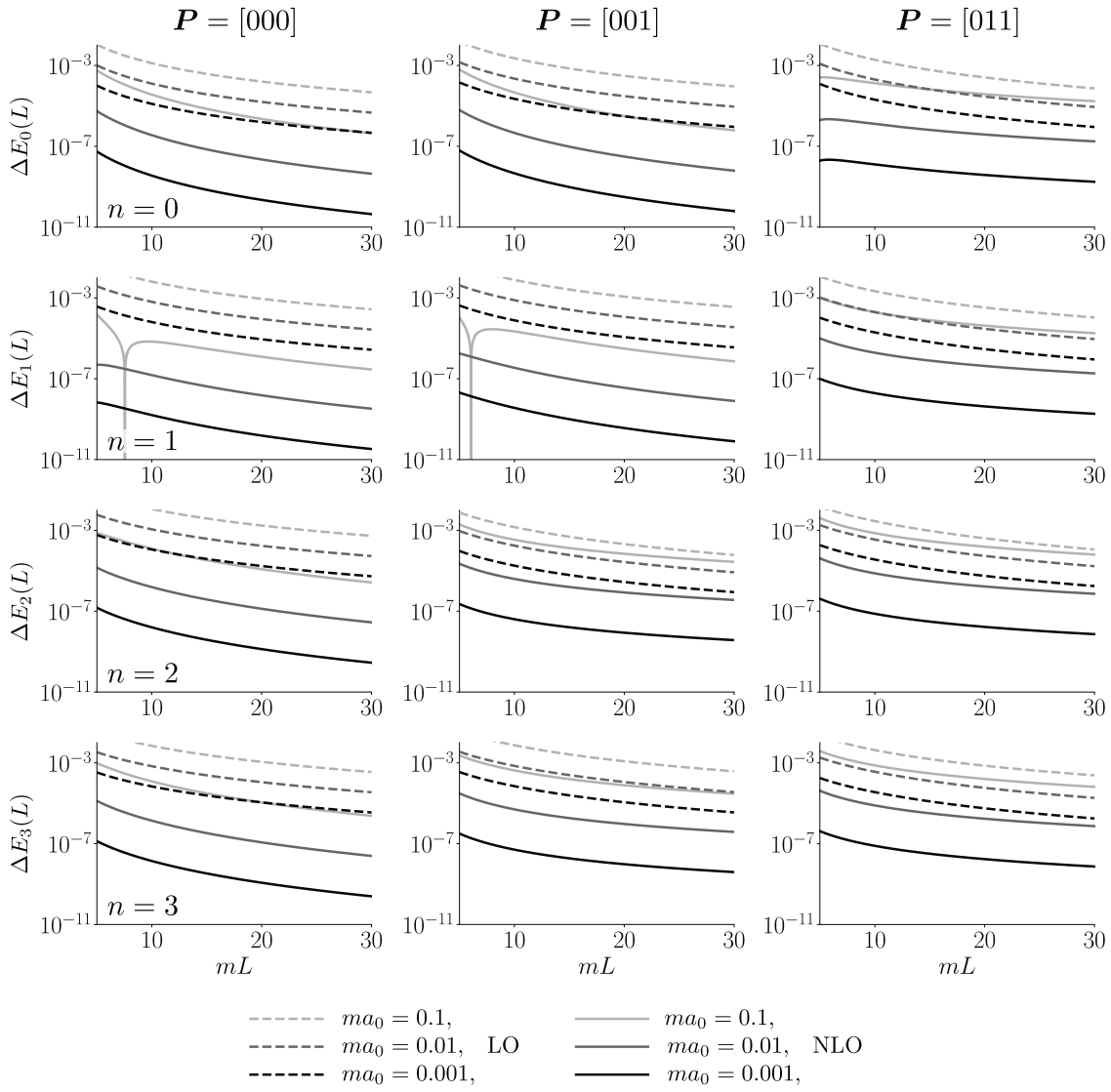

Figure 2. The difference between the full finite-volume energy, found by numerically solving the S-wave-only quantization condition, and the analytic expressions derived in the manuscript. The three columns show three different momenta, $\boldsymbol{P} = [000], [001], [011]$, and the rows show the ground state (top) and first three excited states (second to fourth rows as labeled). Each panel shows three different scattering length values and two orders of subtraction. As expected, the difference decreases when the subtracted order is increased, and smaller values of ma_0 give a smaller residue.

JHEP09(2022)232

In addition to setting the framework for three-particle energies, analytic expressions for two-particle energies are useful in their own right. We have four applications in mind:

First, the results can build intuition on the sensitivity of energy shifts to scattering parameters (e.g. to design a lattice calculation to target a particular scattering observable). This includes basic observations, such as the fact that nonzero total momentum generically reduces the energy shifts and that states with high multiplicity in the non-interacting limit have enhanced shifts.

Second, the expansions may be used to understand volume effects in more complicated lattice quantities, by decomposing the latter in a spectral representation (i.e. inserting a complete set of finite-volume states and then making use of expansions for the energies and matrix elements). This could be instructive, for example, in analyzing volume effects in the vector-vector correlator entering the leading-order hadronic vacuum polarization contribution to the muon's magnetic moment. In particular, excited state expansions may aid in connecting the work of refs. [55, 56] in which volume effects are treated via truncated spectral representations (valid for large current-current separations) to that of refs. [57, 58] in which a large volume expansion is performed for any fixed separation of the vector currents. This is also closely related to the analysis of volume effects for smeared spectral functions discussed, e.g. in refs. [59–63]. In particular in appendix C of ref. [64] an expansion analogous to this work is applied in 1+1 dimensions [see eq. (C16) of that reference] and is used to show that the leading power-like volume effects cancel in the smeared spectral function. The generalization of this to 3+1 dimensions theories is a topic of future work.

Third, the expansions may be useful in designing efficient root finding in numerical solvers of the full quantization condition. This is especially relevant when a given non-interacting energy splits into multiple interacting levels due to accidental degeneracies and, in the three-particle case, when interacting states can cross non-interacting states so that the position of the latter does not always guide the root finder.

Fourth, and finally, the expansions can give information on the convergence of higher partial waves as they enter the finite-volume energies. This is represented by the tables 4–8, which summarize the known geometric part of contribution of the ℓ^{th} partial wave's leading contribution to various energies.

This work clearly opens the door to many generalizations, including expansions of the two-body formalism for non-identical and non-degenerate masses, for multiple channels and for particles with intrinsic spin, as well lifting the restriction to the trivial irrep. Another class of extensions would be to adjust the expansion to accommodate poles in $\tan\delta_\ell(p)$, that generically arise in systems with a narrow resonance. In all cases it should be stressed that an expansion can never contain more information than a direct numerical solution of the quantization condition, provided the later is evaluated with the same angular-momentum truncation and the same scattering amplitudes. Nevertheless, the analytic understanding provided by this approach is highly instructive and will be a useful tool on the way to increasingly ambitious multi-particle lattice calculations.

JHEP09(2022)232

Acknowledgments

We thank Fernando Romero-López and Steve Sharpe for useful discussions. DMG would like to additionally thank Simon Knapen and Michael Wagman for support and useful discussions, and MTH acknowledges Mattia Bruno for useful comments based on presentations of this work in progress. The work of MTH is supported by U.K. Research and Innovation Future Leader Fellowship MR/T019956/1 and in part by U.K. STFC grant ST/P000630/1.

A F function

The geometric function F, for a single channel of identical spin-zero particles, is defined as [10–12, 14]

$$F_{\ell' m',\ell m}(E,\boldsymbol{P},L) = \frac{1}{2}\lim_{\alpha\to 0^+}\left[\frac{1}{L^3}\sum_{\boldsymbol{k}} - \int_{\boldsymbol{k}}\right]\frac{\mathcal{Y}_{\ell' m'}(\boldsymbol{k}^\star)\mathcal{Y}^*_{\ell m}(\boldsymbol{k}^\star)e^{-\alpha(k^{\star 2}-p^{\star 2})}}{2\omega_{\boldsymbol{k}}2\omega_{\boldsymbol{P}-\boldsymbol{k}}(E-\omega_{\boldsymbol{k}}-\omega_{\boldsymbol{P}-\boldsymbol{k}}+i\epsilon)}\,. \tag{A.1}$$

The sum-integral difference is specified using

$$\frac{1}{L^3}\sum_{\boldsymbol{k}} = \frac{1}{L^3}\sum_{\substack{\boldsymbol{k}=2\pi\boldsymbol{v}/L\\ \boldsymbol{v}\in\mathbb{Z}^3}}\,, \qquad \int_{\boldsymbol{k}} = \int\frac{d^3\boldsymbol{k}}{(2\pi)^3}\,, \tag{A.2}$$

where the sum runs over integer-vector multiples of $(2\pi/L)$ and the integral has the usual momentum-space normalization. The various factors of ω are defined via

$$\omega_{\boldsymbol{k}} = \sqrt{m^2+\boldsymbol{k}^2}\,, \qquad \omega_{\boldsymbol{P}-\boldsymbol{k}} = \sqrt{m^2+(\boldsymbol{P}-\boldsymbol{k})^2}\,. \tag{A.3}$$

The CoM frame vector $\boldsymbol{k}^\star$ satisfies

$$\Lambda^\mu{}_\nu(-\boldsymbol{P}/E)\begin{pmatrix}\omega_{\boldsymbol{k}}\\ \boldsymbol{k}\end{pmatrix}^\nu = \begin{pmatrix}\omega^\star_{\boldsymbol{k}}\\ \boldsymbol{k}^\star\end{pmatrix}^\mu\,, \tag{A.4}$$

where $\Lambda^\mu{}_\nu(-\boldsymbol{P}/E)$ is the Lorentz boost with velocity given by the argument, i.e. the boost for which

$$\Lambda^\mu{}_\nu(-\boldsymbol{P}/E)\begin{pmatrix}E\\ \boldsymbol{P}\end{pmatrix}^\nu = \begin{pmatrix}E^\star\\ \boldsymbol{0}\end{pmatrix}^\mu\,. \tag{A.5}$$

We denote the magnitude and direction of $\boldsymbol{k}^\star$ by $k^\star$ and $\hat{\boldsymbol{k}}^\star$, respectively, i.e. $\boldsymbol{k}^\star = k^\star\hat{\boldsymbol{k}}^\star$.

The numerator of eq. (A.1) includes the generalized spherical harmonics

$$\mathcal{Y}_{\ell m}(\boldsymbol{k}^\star) = \sqrt{4\pi}\left(\frac{k^\star}{p^\star}\right)^\ell Y_{\ell m}(\theta^\star,\phi^\star)\,, \tag{A.6}$$

where $p^\star$ is defined in terms of $E^\star$ by eq. (2.6) and the angles defined via $\hat{\boldsymbol{k}}^\star = (\sin\theta^\star\cos\phi^\star, \sin\theta^\star\sin\phi^\star, \cos\theta^\star)$.

The exponential in the numerator of eq. (A.1) is used to regulate the ultraviolet behavior of the sum and integral individually and, as indicated, the regulator independent definition of F is given by sending $\alpha\to 0^+$. Finally, the $i\epsilon$ pole-prescription in F in inherited from

JHEP09(2022)232

the pole-prescription defining the Feynman diagrams appearing in the definition of $\mathcal{M}(E^\star)$ and is also required to make the integral well-defined.

As was shown in refs. [10–12, 14], the F-functions can be rewritten in terms of generalized zeta functions. For example

$$F_{00,00}(E,\boldsymbol{P},L) = \frac{1}{2}\lim_{\alpha\to 0^+}\left[\frac{1}{L^3}\sum_{\boldsymbol{k}} - \int_{\boldsymbol{k}}\right]\frac{e^{-\alpha(k^{\star 2}-p^{\star 2})}}{2\omega_{\boldsymbol{k}}2\omega_{\boldsymbol{P}-\boldsymbol{k}}(E-\omega_{\boldsymbol{k}}-\omega_{\boldsymbol{P}-\boldsymbol{k}}+i\epsilon)}\,, \tag{A.7}$$

$$= \frac{1}{4E^\star}\lim_{\alpha\to 0^+}\left[\frac{1}{L^3}\sum_{\boldsymbol{k}}\frac{\omega^\star_{\boldsymbol{k}}}{\omega_{\boldsymbol{k}}} - \int_{\boldsymbol{k}^\star}\right]\frac{e^{-\alpha(k^{\star 2}-p^{\star 2})}}{p^{\star 2}-\boldsymbol{k}^{\star 2}+i\epsilon}\,, \tag{A.8}$$

$$= \frac{1}{16\pi E^\star}\lim_{s\to -1}\frac{1}{\gamma(q,\boldsymbol{d},L)\,\pi L}\sum_{\boldsymbol{v}\in\mathbb{Z}^3}\Big[q^2-\Gamma(\boldsymbol{v}|q,\boldsymbol{d},L)\Big]^s + i\frac{p^\star}{16\pi E^\star}\,, \tag{A.9}$$

where in the second and third lines we have dropped terms scaling as e^{-mL}. This result, together with

$$\mathcal{M}_{00,00}\,(E^\star)^{-1} = \frac{p^\star\cot\delta_0(p^\star) - ip^\star}{16\pi E^\star}\,, \tag{A.10}$$

implies eq. (2.9) of the main text.

B Level crossing with two-particle energies

In this appendix we show that, while non-interacting two-particle levels never intersect as a function of mL for $\boldsymbol{P}=[000]$, such crossings do occur for non-zero momenta in the finite-volume frame. We also comment on the consequences of this for the definition of the index n, within $\mathfrak{n}=n,\boldsymbol{P},\Lambda$.

The non-crossing for $\boldsymbol{P}=[000]$ follows immediately from the series of inequalities

$$\boldsymbol{\nu}^2_{\mathfrak{n}_2} > \boldsymbol{\nu}^2_{\mathfrak{n}_1} \implies m^2+\frac{4\pi^2}{L^2}\boldsymbol{\nu}^2_{\mathfrak{n}_2} > m^2+\frac{4\pi^2}{L^2}\boldsymbol{\nu}^2_{\mathfrak{n}_1} \implies E_{\mathfrak{n}_2} > E_{\mathfrak{n}_1}\,. \tag{B.1}$$

To see that this breaks for non-zero $\boldsymbol{P}$ consider this particular example for $\boldsymbol{P}=[003]$:

$$E^{(0)}_{2,[003],A_{1g}} = \sqrt{m^2+2\frac{4\pi^2}{L^2}}+\sqrt{m^2+5\frac{4\pi^2}{L^2}}\,, \qquad \Big(\boldsymbol{\nu}_{\mathfrak{n}}=(0,1,1)\Big)\,, \tag{B.2}$$

$$E^{(0)}_{3,[003],A_{1g}} = m+\sqrt{m^2+9\frac{4\pi^2}{L^2}}\,, \qquad \Big(\boldsymbol{\nu}_{\mathfrak{n}}=(0,0,0)\Big)\,, \tag{B.3}$$

where we have explicitly included the ordering index, determined in the large mL limit. The two energies coincide at $mL=3\pi/\sqrt{2}\sim 6.7$. This represents a second kind of accidental degeneracy. Although perturbative results, such as the that given in eq. (2.39), hold on either side of the intersection point, the expansion coefficients become arbitrarily large and diverge as the intersection is approached and thus the expansion breaks down.

Finally, for asymptotically large mL one can use the non-relativistic expansion to show

$$\Big(\boldsymbol{\nu}^2_{\mathfrak{n}_2}+(\boldsymbol{d}-\boldsymbol{\nu}_{\mathfrak{n}_2})^2\Big) > \Big(\boldsymbol{\nu}^2_{\mathfrak{n}_1}+(\boldsymbol{d}-\boldsymbol{\nu}_{\mathfrak{n}_1})^2\Big) \implies E_{\mathfrak{n}_2} > E_{\mathfrak{n}_1}\,, \qquad \Big(L\to\infty\Big)\,, \tag{B.4}$$

i.e. a definitive ordering is restored. This can be used to unambiguously index the energies in studying expansions where such crossings occur.

JHEP09(2022)232

$\boldsymbol{P}$	LG($\boldsymbol{P}$)	N_{elements}	N_{irreps}
$[000]$	O_h	48	10
$[00a]$	C_{4v}	8	5
$[0aa]$	C_{2v}	4	4
$[0ab]$	C_s	2	2
$[aaa]$	C_{3v}	6	3
$[aab]$	C_s	2	2
$[abc]$	C_1	1	1

Table 9. Basic properties of finite-volume little groups for a given $\boldsymbol{P}$, including the name of LG($\boldsymbol{P}$), the number of group elements and the number of irreps. For more details see refs. [11, 12, 53, 54].

C Finite-volume symmetry and projectors

In numerical lattice calculations, one generally considers finite-volume energies in a given irrep of the relevant symmetry group. For a cubic, periodic geometry, the relevant group is determined by the total momentum: for $\boldsymbol{P} = [000]$ the system is invariant under the elements of O_h, the 48-element octahedral group (including parity transformations), while for nonzero $\boldsymbol{P}$ the invariance is reduced to a subgroup of O_h, called the point group or little group and denoted by LG($\boldsymbol{P}$), built from all elements that do not transform the total momentum. In table 9 we list the little groups for all possible total momentum assignments. In order to extract scattering information from lattice results, the quantization condition must also be projected to a fixed irrep, as we have done in eq. (2.2). This is discussed elsewhere in great detail; see for example refs. [11, 12, 53, 54]. Here we only describe a few key points relevant to this work.

Restricting attention first to $\boldsymbol{P} = [000]$, and thus the O_h group, and considering only the trivial irrep A_{1g}, our first aim is to work out the projectors introduced in eq. (2.2), denoted $\mathbb{P}_{A_{1g},\ell m}$ in this case. The defining property of $\mathbb{P}_{A_{1g},\ell m}$ is that, when the m index is contracted with $Y_{\ell m}(\hat{\boldsymbol{k}})$, the resulting function is invariant under the group elements, i.e. for any $R \in O_h$,

$$\sum_m \mathbb{P}_{A_{1g},\ell m} Y_{\ell m}\left(\hat{\boldsymbol{k}}\right) = \sum_m \mathbb{P}_{A_{1g},\ell m} Y_{\ell m}\left(R \cdot \hat{\boldsymbol{k}}\right) , \tag{C.1}$$

where we stress that the sum only runs over m. One can inspect that the following quantity has this property

$$\mathbb{P}_{A_{1g},\ell m} = \frac{1}{\mathcal{N}} \sum_{R \in O_h} Y^*_{\ell m}(R \cdot \hat{\boldsymbol{e}}) , \tag{C.2}$$

where $\mathcal{N}$ is a normalization constant for nonzero vectors and $\hat{\boldsymbol{e}}$ is a generic unit vector. To

JHEP09(2022)232

see that the projector satisfies eq. (C.1), note

$$\sum_m \mathbb{P}_{A_{1g},\ell m} Y_{\ell m}\left(\hat{\boldsymbol{k}}\right) = \sum_m \frac{1}{\mathcal{N}} \sum_{R'\in O_h} Y^*_{\ell m}\left(R'\cdot\hat{\boldsymbol{e}}\right) Y_{\ell m}\left(\hat{\boldsymbol{k}}\right) , \tag{C.3}$$

$$= \frac{2\ell+1}{4\pi}\frac{1}{\mathcal{N}} \sum_{R'\in O_h} P_\ell\left(\hat{\boldsymbol{k}}\cdot R'\cdot\hat{\boldsymbol{e}}\right) , \tag{C.4}$$

$$= \frac{2\ell+1}{4\pi}\frac{1}{\mathcal{N}} \sum_{R''\in O_h} P_\ell\left(\hat{\boldsymbol{k}}\cdot R\cdot R''\cdot\hat{\boldsymbol{e}}\right) , \tag{C.5}$$

$$= \sum_m \mathbb{P}_{A_{1g},\ell m} Y_{\ell m}\left(R\cdot\hat{\boldsymbol{k}}\right) . \tag{C.6}$$

Similar relations can be used to prove

$$|\mathcal{N}|^2 = |O_h| \sum_{R\in O_h}\sum_m Y^*_{\ell m}\left(R\cdot\hat{\boldsymbol{e}}\right) Y_{\ell m}\left(\hat{\boldsymbol{e}}\right) . \tag{C.7}$$

As an example, applying this for $\ell = 4$ gives

$$\mathbb{P}_{A_{1g},4m'} = \frac{1}{2\sqrt{6}}\left(\sqrt{5},0,0,0,\sqrt{14},0,0,0,\sqrt{5}\right)_{m'} . \tag{C.8}$$

This is then used to define f_{40} and f_{44}, used in section 2.5.

To make this useful for general ℓ we return to the expressions of section 2.5, beginning with the definition of $M_{\ell\ell'}$, eq. (2.44), which we repeat for convenience

$$M^{\mathfrak{n}}_{\ell\ell'} = 4\pi \mathbb{P}_{A_{1g},\ell m}\, \mathbb{P}_{A_{1g},\ell' m'} \frac{1}{|O_h|} \sum_{R\in O_h} Y_{\ell m}\left(R\cdot\hat{\boldsymbol{\nu}}_{\mathfrak{n}}\right) Y^*_{\ell' m'}\left(R\cdot\hat{\boldsymbol{\nu}}_{\mathfrak{n}}\right) , \tag{C.9}$$

where we recall that $\boldsymbol{\nu}_{\mathfrak{n}}$, defined in and after eq. (2.8), is an integer vector representing the $\mathfrak{n}^{\text{th}}$ non-interacting state. Now note that, because of eq. (C.1), the sum over rotations is redundant and thus

$$M^{\mathfrak{n}}_{\ell\ell'} = 4\pi \mathbb{P}_{A_{1g},\ell m}\, \mathbb{P}_{A_{1g},\ell' m'} Y_{\ell m}(\hat{\boldsymbol{\nu}}_{\mathfrak{n}}) Y^*_{\ell' m'}(\hat{\boldsymbol{\nu}}_{\mathfrak{n}}) . \tag{C.10}$$

From this it is clear that $M^{\mathfrak{n}}_{\ell\ell'}$ is rank one: we write $M^{\mathfrak{n}}_{\ell\ell'} = \sqrt{\mathcal{P}_\ell}\sqrt{\mathcal{P}_{\ell'}}$ where

$$\mathcal{P}_\ell = 4\pi\left(\mathbb{P}_{A_{1g},\ell m} Y_{\ell m}(\hat{\boldsymbol{\nu}}_{\mathfrak{n}})\right)^2 . \tag{C.11}$$

Finally substituting our expression for the projector yields

$$\mathcal{P}_\ell = 4\pi\left(\frac{1}{\mathcal{N}}\sum_m \sum_{R\in O_h} Y^*_{\ell m}\left(R\cdot\hat{\boldsymbol{e}}\right) Y_{\ell m}\left(\hat{\boldsymbol{\nu}}_{\mathfrak{n}}\right)\right)^2 , \tag{C.12}$$

$$= 4\pi\left(|O_h|\sum_{R\in O_h}\sum_m Y^*_{\ell m}\left(R\cdot\hat{\boldsymbol{e}}\right) Y_{\ell m}\left(\hat{\boldsymbol{e}}\right)\right)^{-1}\left(\sum_m\sum_{R\in O_h} Y^*_{\ell m}\left(R\cdot\hat{\boldsymbol{e}}\right) Y_{\ell m}\left(\hat{\boldsymbol{\nu}}_{\mathfrak{n}}\right)\right)^2 . \tag{C.13}$$

where in the second line we have substituted the result for $\mathcal{N}$, eq. (C.7).

JHEP09(2022)232

At this point, a few comments are in order about the arbitrary vector $\hat{\boldsymbol{e}}$ in eq. (C.2). To fully specify the role of this vector we take a small detour over some basics of groups and representations. While ℓ specifies an irrep of the group of continuous rotations SO(3), it is no longer irreducible with respect to the subgroup of the finite volume system. Instead, a given ℓ value splits into a set of finite-volume irreps. This manifests in the quantization condition by the fact that finite-volume energies in the given irrep are shifted by the partial wave. For the case of O_h, the symmetry group of $\boldsymbol{P} = [000]$, all even ℓ besides $\ell = 2$ contain at least one embedding of the trivial irrep. In addition, while exactly one embedding occurs for $\ell = 0, 4, 6$ and 10, for $\ell = 12$ and some other higher values, multiple embeddings can arise.

Consider first the values of ℓ for which exactly one embedding appears. Then $\mathbb{P}_{A_{1g},\ell m}$ must be uniquely specified up to a phase and any choice of $\hat{\boldsymbol{e}}$ will give the same result, up to that ambiguity. Within the definition of $\mathcal{P}_\ell$, it is particularly convenient to choose $\hat{\boldsymbol{e}} = \hat{\boldsymbol{\nu}}_{\mathfrak{n}}$, from which follows

$$\mathcal{P}_\ell = 4\pi \frac{1}{|O_h|} \sum_{R \in O_h} \sum_m Y^*_{\ell m}(R \cdot \hat{\boldsymbol{k}}) Y_{\ell m}(\hat{\boldsymbol{\nu}}_{\mathfrak{n}}) \,, \tag{C.14}$$

$$= (2\ell + 1) \frac{1}{|O_h|} \sum_{R \in O_h} P_\ell(\hat{\boldsymbol{\nu}}_{\mathfrak{n}} \cdot R \cdot \hat{\boldsymbol{\nu}}_{\mathfrak{n}}) \,. \tag{C.15}$$

This matches eq. (2.46) of the main text.

Next consider a case such as $\ell = 12$, for which multiple embeddings of the trivial irrep appear. Provided the state of interest does not exhibit an accidental degeneracy, one can show that using eq. (C.15) still gives the correct result for the leading-order shift. To prove this generally, suppose that a given ℓ value has $K > 1$ embeddings of A_{1g} forming a basis of vectors $\mathbb{P}_{A_{1g}(1),\ell m}, \mathbb{P}_{A_{1g}(2),\ell m}, \cdots, \mathbb{P}_{A_{1g}(K),\ell m}$. Choose $\mathbb{P}_{A_{1g}(1),\ell m}$ as the vector generated by $\hat{\boldsymbol{e}} = \hat{\boldsymbol{\nu}}_{\mathfrak{n}}$. Next note that, since the projectors are orthonormal, for any $k \neq 1$ one has

$$\sum_m \mathbb{P}_{A_{1g}(k),\ell m} \mathbb{P}^*_{A_{1g}(1),\ell m} = \frac{1}{\mathcal{N}} \sum_m \mathbb{P}_{A_{1g}(k),\ell m} \sum_{R \in O_h} Y_{\ell m}(R \cdot \hat{\boldsymbol{\nu}}_{\mathfrak{n}}) = 0 \,. \tag{C.16}$$

This implies that $\mathbb{P}_{A_{1g}(k),\ell m}$ annihilates the expression for $F_{\ell m,\ell' m'}$, expanded to leading-order about the non-accidentally degenerate state of interest, meaning that no solution appears for the given state and embedding. For states with an accidental degeneracy, by contrast, one must keep the full subspace spanned by $\mathbb{P}_{A_{1g}(1),\ell m}, \mathbb{P}_{A_{1g}(2),\ell m}, \cdots, \mathbb{P}_{A_{1g}(K),\ell m}$ to identify the complete set of interacting solutions. For the rest frame this is a highly obscure case, since it requires $\ell = 12$ or higher and the first accidentally degenerate state is the 8^{th} excited state.

These results generalize readily to nonzero $\boldsymbol{P}$ with A_{1g} replaced by A_1, the label of the trivial irrep for all groups besides O_h. As with the rest frame case, the key observation is that

$$\mathbb{P}_{A_1,\ell m} = \frac{1}{\mathcal{N}} \sum_{R \in \mathrm{LG}(\boldsymbol{P})} Y^*_{\ell m}(R \cdot \hat{\boldsymbol{\nu}}^\star_{\mathfrak{n}}) \,, \tag{C.17}$$

defines a generic projector that can be used to derive the contribution of all partial waves to the leading-order energy shift.

JHEP09(2022)232

D Equivalence of poles and non-interacting energies

In this appendix we show that the set of $\boldsymbol{v}$ solving

$$q^2 - \Gamma(\boldsymbol{v}|q, \boldsymbol{d}, L) = 0\,, \tag{D.1}$$

exactly corresponds to the set satisfying

$$E = \omega_{\boldsymbol{v}} + \omega_{\boldsymbol{d}-\boldsymbol{v}}\,, \tag{D.2}$$

provided that $E^\star > 0$.

As a first step we follow ref. [14] to write

$$q^2 - \Gamma(\boldsymbol{v}|q, \boldsymbol{d}, L) = q^2 - \frac{1}{\gamma(q, \boldsymbol{d}, L)^2}\left(\boldsymbol{v}_\parallel - \frac{\boldsymbol{d}}{2}\right)^2 - \boldsymbol{v}_\perp^2\,, \tag{D.3}$$

$$= (E^\star/2 - \omega_{\boldsymbol{v}}^\star) \times \Xi(\boldsymbol{v}, E, \boldsymbol{d}, L)\,, \tag{D.4}$$

where $\boldsymbol{v}_\parallel$ and $\boldsymbol{v}_\perp$ are the components of $\boldsymbol{v}$ that are parallel and perpendicular to $\boldsymbol{d}$, respectively. In the second line we have introduced

$$\Xi(\boldsymbol{v}^\star, E, \boldsymbol{d}, L) \equiv \frac{L^2}{4\pi^2}\left(E^\star/2 + \omega_{\boldsymbol{v}}^\star\right) + 2\frac{\boldsymbol{d}}{E}\cdot\boldsymbol{v}^\star - \frac{\boldsymbol{d}^2}{E^2}\left(E^\star/2 - \omega_{\boldsymbol{v}}^\star\right)\,, \tag{D.5}$$

$$= \frac{L^2}{4\pi^2}\left[\frac{E^\star}{2}\left(1 - \boldsymbol{\beta}^2\right) + \frac{4\pi}{L}\boldsymbol{\beta}\cdot\boldsymbol{v}^\star + \omega_{\boldsymbol{v}}^\star(1 + \boldsymbol{\beta}^2)\right]\,. \tag{D.6}$$

The result (D.4), derived in ref. [14], together with the fact that Ξ is finite for all finite values of its arguments (and nonzero L) is enough to show that a solution of $E^\star - 2\omega_{\boldsymbol{v}}^\star = 0$ also satisfies $q^2 - \Gamma = 0$.

To show the converse, that a solution of $q^2 - \Gamma = 0$ also satisfies $E^\star - 2\omega_{\boldsymbol{v}}^\star = 0$, we now prove that Ξ cannot vanish for $E^\star > 0$. This can be achieved by demonstrating the inequality

$$-2\boldsymbol{\beta}\cdot\boldsymbol{k}^\star - \omega_{\boldsymbol{v}}^\star\left(1 + \boldsymbol{\beta}^2\right) < \frac{E^\star}{2}\left(1 - \boldsymbol{\beta}^2\right)\,, \tag{D.7}$$

where we have defined $\boldsymbol{k}^\star \equiv 2\pi\boldsymbol{v}^\star/L$. This, in turn, can be demonstrated via

$$-2\boldsymbol{\beta}\cdot\boldsymbol{k}^\star < \omega_{\boldsymbol{v}}^\star\left(1 + \boldsymbol{\beta}^2\right)\,, \tag{D.8}$$

which is a stronger result since $1 - \boldsymbol{\beta}^2 > 0$. To see that (D.8) holds, note that the left-hand side is maximized when $-2\boldsymbol{\beta}\cdot\boldsymbol{k}^\star = 2|\boldsymbol{\beta}||\boldsymbol{k}^\star|$. Squaring both sides gives

$$4\boldsymbol{k}^{\star 2} < (m^2 + \boldsymbol{k}^{\star 2})\frac{\left(1 + \boldsymbol{\beta}^2\right)^2}{\boldsymbol{\beta}^2}\,, \tag{D.9}$$

which holds since $x + 1/x > 2$ for $x \in [0, 1)$. It follows that $\Xi \neq 0$ for all real values of its arguments, provided $E^\star > 0$.

Having shown that the set satisfying $q^2 - \Gamma = 0$ is equivalent to that satisfying $E^\star - 2\omega_{\boldsymbol{v}}^\star = 0$, it remains only to prove that the latter is also equivalent to the set of $\boldsymbol{v}$

JHEP09(2022)232

satisfying the moving frame condition: $E - \omega_{\boldsymbol{v}} - \omega_{\boldsymbol{d}-\boldsymbol{v}} = 0$. This is the case, due to the fact that the following expressions have the same set of roots for $E^\star > 0$

$$\begin{aligned} E^\star - 2\omega_{\boldsymbol{v}}^\star &\Leftrightarrow (E^\star - \omega_{\boldsymbol{v}}^\star + \omega_{\boldsymbol{v}}^\star)(E^\star - 2\omega_{\boldsymbol{v}}^\star)\,, && \text{(D.10)} \\ &\Leftrightarrow (E^\star - \omega_{\boldsymbol{v}}^\star)^2 - \boldsymbol{k}^{\star 2} - m^2\,, && \text{(D.11)} \\ &\Leftrightarrow (P-k)^2 - m^2\,, && \text{(D.12)} \\ &\Leftrightarrow (E - \omega_{\boldsymbol{v}} - \omega_{\boldsymbol{d}-\boldsymbol{v}})(E - \omega_{\boldsymbol{v}} + \omega_{\boldsymbol{d}-\boldsymbol{v}})\,, && \text{(D.13)} \end{aligned}$$

where $\Leftrightarrow$ is used here to indicate that the two expressions have the same roots. Here we have introduced $P^{\star\mu} = (E^\star, \boldsymbol{0})$ and $k^{\star\mu} = (\omega_{\boldsymbol{v}}^\star, \boldsymbol{k}^\star)$ and used the fact that $(P-k)^2$ is a Lorentz scalar to rewrite it in the finite-volume frame.

Finally, to see that the unwanted factor in the final line does not induce any additional solutions, note that it has the same roots as the following:

$$\begin{aligned} E - \omega_{\boldsymbol{v}} + \omega_{\boldsymbol{d}-\boldsymbol{v}} &\Leftrightarrow (E - \omega_{\boldsymbol{v}} + \omega_{\boldsymbol{d}-\boldsymbol{v}})(E + \omega_{\boldsymbol{v}} + \omega_{\boldsymbol{d}-\boldsymbol{v}}) && \text{(D.14)} \\ &\Leftrightarrow (E + \omega_{\boldsymbol{v}'})^2 - \omega_{\boldsymbol{d}-\boldsymbol{v}'}^2 && \text{(D.15)} \\ &\Leftrightarrow (P + k')^2 - m^2\,, && \text{(D.16)} \\ &\Leftrightarrow (E^\star + \omega_{\boldsymbol{k}}'^\star)^2 - \omega_{\boldsymbol{k}}'^{\star 2}\,, && \text{(D.17)} \\ &\Leftrightarrow E^\star(E^\star + 2\omega_{\boldsymbol{k}}'^\star)\,, && \text{(D.18)} \end{aligned}$$

where we have introduced $\boldsymbol{v}' = \boldsymbol{d} - \boldsymbol{v}$ and $k'^\mu = (\omega_{\boldsymbol{k}}', -2\pi\boldsymbol{v}'/L)$. The final expression is manifestly nonzero for $E^\star > 0$. This completes the proof.

E Two observations concerning accidental degeneracy

In this appendix, we prove the assertions given in section 2.6.

We begin by demonstrating that, for total momentum types $\boldsymbol{P} = [00a]$ and $\boldsymbol{P} = [aaa]$, accidental degeneracies in the trivial irrep are only broken when $\ell = 4$ is included, even though $\ell = 2$ contributes to the energies. We also show the converse, that for all other non-zero total momenta the degeneracy is broken by $\ell = 2$.

Before turning to the various cases in the moving frame, we review the situation for $\boldsymbol{P} = [000]$. Here $\ell = 4$ is the first non-trivial partial wave that contributes to trivial-irrep energies and, as we discuss in section 2.6, including this partial wave does indeed split the accidentally degenerate states. The splitting occurs because the matrix $f_{\ell\ell'}$, truncated to $\ell_{\mathsf{max}} = 4$ and then expanded to leading order about the non-interacting solution, has rank exceeding one whenever the solution of interest is accidentally degenerate.

The condition that the truncated and expanded $f_{\ell\ell'}$ is rank one is equivalent to the relation

$$\sum_{m=-\ell}^{\ell} \mathbb{P}_{A_1 g, \ell m} Y_{\ell m}(\hat{\boldsymbol{\nu}}_{\mathfrak{n}}) = \sum_{m=-\ell}^{\ell} \mathbb{P}_{A_1 g, \ell m} Y_{\ell m}(\hat{\boldsymbol{v}})\,, \qquad \forall\, \boldsymbol{v} \in \boldsymbol{S}_{\mathfrak{n}}\,, \tag{E.1}$$

and this holds for the low lying states, for which all elements of $\boldsymbol{S}_{\mathfrak{n}}$ are rotations of $\boldsymbol{\nu}_{\mathfrak{n}}$, but generally fails at $\ell = 4$ whenever an accidental degeneracy occurs. For example, one can

JHEP09(2022)232

readily check that the left-hand side gives different values when evaluated at $\boldsymbol{\nu}_{\mathfrak{n}} = (0,0,3)$ as compared to $\boldsymbol{\nu}_{\mathfrak{n}} = (1,2,2)$. Since both of these three-vectors are within $\boldsymbol{S}_{\mathfrak{n}}$ for the 8^{th} excited state, this is sufficient.

Returning to non-zero $\boldsymbol{P}$, note that $\boldsymbol{\nu}_{\mathfrak{n}}$ and $\boldsymbol{\nu}'_{\mathfrak{n}}$ represent degenerate states if and only if

$$\omega_{\boldsymbol{\nu}_{\mathfrak{n}}} + \omega_{\boldsymbol{d}-\boldsymbol{\nu}_{\mathfrak{n}}} = \omega_{\boldsymbol{\nu}'_{\mathfrak{n}}} + \omega_{\boldsymbol{d}-\boldsymbol{\nu}'_{\mathfrak{n}}}\,, \tag{E.2}$$

but $\boldsymbol{\nu}_{\mathfrak{n}}$ cannot be transformed into either $\boldsymbol{\nu}'_{\mathfrak{n}}$ or $\boldsymbol{d} - \boldsymbol{\nu}'_{\mathfrak{n}}$ via an element of the little group, $\mathrm{LG}(\boldsymbol{P})$.

Next, defining $\boldsymbol{\nu}^\star_{\mathfrak{n}}$ as the result of boosting $(L\omega_{\boldsymbol{\nu}_{\mathfrak{n}}}/(2\pi), \boldsymbol{\nu}_{\mathfrak{n}})$ with velocity $\boldsymbol{\beta} = -\boldsymbol{P}/(\omega_{\boldsymbol{\nu}_{\mathfrak{n}}} + \omega_{\boldsymbol{d}-\boldsymbol{\nu}_{\mathfrak{n}}})$, we see that eq. (E.2) implies

$$2\omega_{\boldsymbol{\nu}^\star_{\mathfrak{n}}} = 2\omega_{\boldsymbol{\nu}'^\star_{\mathfrak{n}}}\,, \tag{E.3}$$

and thus[3]

$$(\boldsymbol{\nu}^\star_\perp)^2 + (\boldsymbol{\nu}^\star_\parallel)^2 = (\boldsymbol{\nu}'^\star_\perp)^2 + (\boldsymbol{\nu}'^\star_\parallel)^2\,, \tag{E.4}$$

where $\boldsymbol{\nu}^\star_\perp$ and $\boldsymbol{\nu}^\star_\parallel$ are three-vectors parallel and perpendicular to $\boldsymbol{d}$ satisfying $\boldsymbol{\nu}^\star = \boldsymbol{\nu}^\star_\perp + \boldsymbol{\nu}^\star_\parallel$. Because $\boldsymbol{\nu}^\star_\parallel$ and $\boldsymbol{\nu}'^\star_\parallel$ are boost dependent, while $\boldsymbol{\nu}^\star_\perp = \boldsymbol{\nu}_\perp$ and $\boldsymbol{\nu}'^\star_\perp = \boldsymbol{\nu}'_\perp$ are not, one can additionally infer

$$(\boldsymbol{\nu}^\star_\perp)^2 = (\boldsymbol{\nu}'^\star_\perp)^2\,, \qquad\qquad (\boldsymbol{\nu}^\star_\parallel)^2 = (\boldsymbol{\nu}'^\star_\parallel)^2\,. \tag{E.5}$$

We are now in position to determine whether the $\ell = 2$ partial wave will lead to a splitting in the corresponding energies. As with the rest-frame case, a splitting will occur whenever the $f_{\ell\ell'}$ matrix, truncated to $\ell_{\mathsf{max}} = 2$ and expanded about the state of interest, has a rank exceeding one. This, in turn, occurs whenever

$$\sum_{m=-2}^{2} \mathbb{P}_{A_1,2m} Y_{2m}(\hat{\boldsymbol{\nu}}^\star) \neq \sum_{m=-2}^{2} \mathbb{P}_{A_1,2m} Y_{2m}(\hat{\boldsymbol{\nu}}'^\star)\,, \tag{E.6}$$

where $\mathbb{P}_{A_1,\ell m}$ is a projector to the trivial irrep of $\mathrm{LG}(\boldsymbol{P})$.

To explore this condition we require some additional notation. We define $\nu^\star_{\parallel,z} = \hat{\boldsymbol{d}} \cdot \boldsymbol{\nu}^\star_\parallel$ as the component of $\nu^\star_\parallel$ along the momentum direction. Note that this is equal to $|\boldsymbol{\nu}^\star_\parallel|$ up to a sign. Here we include the z-subscript to suggest the definition of a coordinate system with the z-axis along $\boldsymbol{d}$. Similarly we introduce $(\nu^\star_{\perp,x}, \nu^\star_{\perp,y})$ as the two components of $\boldsymbol{\nu}^\star_\perp$ along two arbitrary axes perpendicular to $\boldsymbol{d}$. With these components in hand the sum over the $\ell = 2$ harmonics takes the form

$$\begin{aligned}|\boldsymbol{\nu}^\star|^2 \sum_{m=-\ell}^{\ell} \mathbb{P}_{A_1,\ell m} Y_{\ell m}(\hat{\boldsymbol{\nu}}^\star) = \alpha_1 \left[(\nu^\star_{\perp,x})^2 + (\nu^\star_{\perp,y})^2\right] + \alpha_2 (\nu^\star_{\parallel,z})^2 \\ + \beta_1 \left[(\nu^\star_{\perp,x})^2 - (\nu^\star_{\perp,y})^2\right] + \beta_2 \nu^\star_{\perp,x}\nu^\star_{\perp,y} + \beta_3 \nu^\star_{\parallel,z}\nu^\star_{\perp,x} + \beta_4 \nu^\star_{\parallel,z}\nu^\star_{\perp,x}\,,\end{aligned} \tag{E.7}$$

where α_1, α_2, β_1, β_2, β_3, and β_4 are coefficients that depend on $\boldsymbol{d}$ and on the exact definition of $\mathbb{P}_{A_1,2m}$. Combining eqs. (E.5), (E.6) and (E.7), we deduce that the $\ell = 2$ partial wave cannot break accidental degeneracies if, for a given $\boldsymbol{P}$, $\beta_i = 0$. Thus it remains only

[3] To avoid clutter of notation we drop the $\mathfrak{n}$ subscript for the remainder of this appendix.

JHEP09(2022)232

to show that this is the case for $\boldsymbol{P} = [00a]$ and $\boldsymbol{P} = [aaa]$ but not for other values of total momentum.

The terms multiplying β_i coefficients are all symmetry breaking, i.e. are not invariant under continuous rotations about the $\boldsymbol{d}$ axis. At the same time, because $\mathbb{P}_{A_1,\ell m}$ projects to the trivial irrep, $\sum_m \mathbb{P}_{A_1,\ell m} Y_{\ell m}(\hat{\boldsymbol{\nu}}^\star)$ must be invariant under the group elements, by construction. This gives a number of constraints on the coefficients, and it follows that $\beta_i = 0$ whenever the little group, $\mathrm{LG}(\boldsymbol{P})$, is large enough to give the required constraints. In the case of $\boldsymbol{P} = [00a]$ one can readily identify the required symmetries

$$\nu^\star_{\perp,x} \leftrightarrow \nu^\star_{\perp,y} \quad \Rightarrow \quad \beta_1 = 0,\ \beta_3 = \beta_4\,, \tag{E.8}$$

$$\nu^\star_{\perp,x} \leftrightarrow -\nu^\star_{\perp,x}\,,\ \nu^\star_{\perp,y} \leftrightarrow -\nu^\star_{\perp,y} \quad \Rightarrow \quad \beta_3 = \beta_4 = 0\,, \tag{E.9}$$

$$\nu^\star_{\perp,x} \leftrightarrow -\nu^\star_{\perp,x} \quad \Rightarrow \quad \beta_2 = 0\,. \tag{E.10}$$

Similarly for $\boldsymbol{P} = [aaa]$ one can identify constraints from the six elements of the corresponding little group that ensure $\beta_i = 0$. To complete the demonstration one must find examples of all other nonzero momentum types, namely types $[0aa]$, $[0ab]$, $[abb]$, $[abc]$, for which the β_i coefficients are non-zero. We have done this through explicit calculation and have confirmed that whenever accidental degeneracy occurs, it is broken by the $\ell = 2$ harmonics. Note that this is highly plausible given the results of table 9. Each of the symmetry groups for which $\ell = 2$ generates the splittings has 4 or fewer elements, meaning that not enough constraints arise to require $\beta_i = 0$.

We now turn to the second claim presented in section 2.6 that, in the limit where the coefficients of higher partial waves are taken arbitrarily small, one of the states in an accidentally degenerate system is shifted according to the naive result

$$\Delta^{(1)}_{E[\mathfrak{n}],+}(L) = g_{\mathfrak{n}} \frac{E^{(0)}_{\mathfrak{n}}(L)}{4\omega_{\boldsymbol{\nu}_{\mathfrak{n}}}\omega_{\boldsymbol{d}-\boldsymbol{\nu}_{\mathfrak{n}}}} \frac{8\pi a_0}{\gamma^{(0)}_{\mathfrak{n}} L^3}\,. \tag{E.11}$$

This follows directly from noting that the roots of eq. (2.41) (with the $\ell = 4$ replaced by a generic ℓ) match those of the following relation:

$$\left[1 - f_{00}(q,\boldsymbol{d},L)\frac{\tan\delta_0(p)}{p}\right]\left[1 - f_{\ell\ell}(q,\boldsymbol{d},L)\frac{\tan\delta_\ell(p)}{p}\right] = f_{\ell 0}(q,\boldsymbol{d},L)^2 \frac{\tan\delta_0(p)\tan\delta_\ell(p)}{p^2}\,. \tag{E.12}$$

As $\delta_\ell(p)$ tends to zero this manifestly picks up the solution of eq. (2.9) together with non-interacting solutions.

References

[1] R.A. Briceno, J.J. Dudek and R.D. Young, *Scattering processes and resonances from lattice QCD*, *Rev. Mod. Phys.* **90** (2018) 025001 [arXiv:1706.06223] [INSPIRE].

[2] J. Bulava, *Meson-Nucleon Scattering Amplitudes from Lattice QCD*, *AIP Conf. Proc.* **2249** (2020) 020006 [arXiv:1909.13097] [INSPIRE].

JHEP09(2022)232

[3] USQCD collaboration, *Hadrons and Nuclei*, *Eur. Phys. J. A* **55** (2019) 193 [arXiv:1904.09512] [INSPIRE].

[4] R.G. Edwards, *Hadron Spectroscopy*, *PoS* **LATTICE2019** (2020) 253 [INSPIRE].

[5] RBC and UKQCD collaborations, *$K \to \pi\pi$ decay, ε' and the RBC-UKQCD kaon physics program*, *J. Phys. Conf. Ser.* **1526** (2020) 012012 [INSPIRE].

[6] S. Aoki and T. Doi, *Lattice QCD and baryon-baryon interactions: HAL QCD method*, *Front. in Phys.* **8** (2020) 307 [arXiv:2003.10730] [INSPIRE].

[7] M.T. Hansen and S.R. Sharpe, *Lattice QCD and Three-particle Decays of Resonances*, *Ann. Rev. Nucl. Part. Sci.* **69** (2019) 65 [arXiv:1901.00483] [INSPIRE].

[8] A. Rusetsky, *Three particles on the lattice*, *PoS* **LATTICE2019** (2019) 281 [arXiv:1911.01253] [INSPIRE].

[9] M. Mai, M. Döring and A. Rusetsky, *Multi-particle systems on the lattice and chiral extrapolations: a brief review*, *Eur. Phys. J. ST* **230** (2021) 1623 [arXiv:2103.00577] [INSPIRE].

[10] M. Lüscher, *Volume Dependence of the Energy Spectrum in Massive Quantum Field Theories. 2. Scattering States*, *Commun. Math. Phys.* **105** (1986) 153 [INSPIRE].

[11] M. Lüscher, *Two particle states on a torus and their relation to the scattering matrix*, *Nucl. Phys. B* **354** (1991) 531 [INSPIRE].

[12] K. Rummukainen and S.A. Gottlieb, *Resonance scattering phase shifts on a nonrest frame lattice*, *Nucl. Phys. B* **450** (1995) 397 [hep-lat/9503028] [INSPIRE].

[13] S. He, X. Feng and C. Liu, *Two particle states and the S-matrix elements in multi-channel scattering*, *JHEP* **07** (2005) 011 [hep-lat/0504019] [INSPIRE].

[14] C.h. Kim, C.T. Sachrajda and S.R. Sharpe, *Finite-volume effects for two-hadron states in moving frames*, *Nucl. Phys. B* **727** (2005) 218 [hep-lat/0507006] [INSPIRE].

[15] M. Lage, U.-G. Meissner and A. Rusetsky, *A Method to measure the antikaon-nucleon scattering length in lattice QCD*, *Phys. Lett. B* **681** (2009) 439 [arXiv:0905.0069] [INSPIRE].

[16] V. Bernard, M. Lage, U.G. Meissner and A. Rusetsky, *Scalar mesons in a finite volume*, *JHEP* **01** (2011) 019 [arXiv:1010.6018] [INSPIRE].

[17] Z. Fu, *Rummukainen-Gottlieb's formula on two-particle system with different mass*, *Phys. Rev. D* **85** (2012) 014506 [arXiv:1110.0319] [INSPIRE].

[18] M.T. Hansen and S.R. Sharpe, *Multiple-channel generalization of Lellouch-Lüscher formula*, *Phys. Rev. D* **86** (2012) 016007 [arXiv:1204.0826] [INSPIRE].

[19] R.A. Briceno and Z. Davoudi, *Moving multichannel systems in a finite volume with application to proton-proton fusion*, *Phys. Rev. D* **88** (2013) 094507 [arXiv:1204.1110] [INSPIRE].

[20] P. Guo, J. Dudek, R. Edwards and A.P. Szczepaniak, *Coupled-channel scattering on a torus*, *Phys. Rev. D* **88** (2013) 014501 [arXiv:1211.0929] [INSPIRE].

[21] R.A. Briceno, *Two-particle multichannel systems in a finite volume with arbitrary spin*, *Phys. Rev. D* **89** (2014) 074507 [arXiv:1401.3312] [INSPIRE].

[22] R.A. Briceno and Z. Davoudi, *Three-particle scattering amplitudes from a finite volume formalism*, *Phys. Rev. D* **87** (2013) 094507 [arXiv:1212.3398] [INSPIRE].

JHEP09(2022)232

[23] K. Polejaeva and A. Rusetsky, *Three particles in a finite volume*, *Eur. Phys. J. A* **48** (2012) 67 [arXiv:1203.1241] [INSPIRE].

[24] M.T. Hansen and S.R. Sharpe, *Relativistic, model-independent, three-particle quantization condition*, *Phys. Rev. D* **90** (2014) 116003 [arXiv:1408.5933] [INSPIRE].

[25] M.T. Hansen and S.R. Sharpe, *Expressing the three-particle finite-volume spectrum in terms of the three-to-three scattering amplitude*, *Phys. Rev. D* **92** (2015) 114509 [arXiv:1504.04248] [INSPIRE].

[26] R.A. Briceño, M.T. Hansen and S.R. Sharpe, *Relating the finite-volume spectrum and the two-and-three-particle S matrix for relativistic systems of identical scalar particles*, *Phys. Rev. D* **95** (2017) 074510 [arXiv:1701.07465] [INSPIRE].

[27] H.-W. Hammer, J.-Y. Pang and A. Rusetsky, *Three-particle quantization condition in a finite volume: 1. The role of the three-particle force*, *JHEP* **09** (2017) 109 [arXiv:1706.07700] [INSPIRE].

[28] H.W. Hammer, J.Y. Pang and A. Rusetsky, *Three particle quantization condition in a finite volume: 2. general formalism and the analysis of data*, *JHEP* **10** (2017) 115 [arXiv:1707.02176] [INSPIRE].

[29] M. Mai and M. Döring, *Three-body Unitarity in the Finite Volume*, *Eur. Phys. J. A* **53** (2017) 240 [arXiv:1709.08222] [INSPIRE].

[30] R.A. Briceño, M.T. Hansen and S.R. Sharpe, *Three-particle systems with resonant subprocesses in a finite volume*, *Phys. Rev. D* **99** (2019) 014516 [arXiv:1810.01429] [INSPIRE].

[31] R.A. Briceño, M.T. Hansen and S.R. Sharpe, *Numerical study of the relativistic three-body quantization condition in the isotropic approximation*, *Phys. Rev. D* **98** (2018) 014506 [arXiv:1803.04169] [INSPIRE].

[32] A.W. Jackura et al., *Equivalence of three-particle scattering formalisms*, *Phys. Rev. D* **100** (2019) 034508 [arXiv:1905.12007] [INSPIRE].

[33] T.D. Blanton, F. Romero-López and S.R. Sharpe, *Implementing the three-particle quantization condition including higher partial waves*, *JHEP* **03** (2019) 106 [arXiv:1901.07095] [INSPIRE].

[34] R.A. Briceño, M.T. Hansen, S.R. Sharpe and A.P. Szczepaniak, *Unitarity of the infinite-volume three-particle scattering amplitude arising from a finite-volume formalism*, *Phys. Rev. D* **100** (2019) 054508 [arXiv:1905.11188] [INSPIRE].

[35] F. Romero-López, S.R. Sharpe, T.D. Blanton, R.A. Briceño and M.T. Hansen, *Numerical exploration of three relativistic particles in a finite volume including two-particle resonances and bound states*, *JHEP* **10** (2019) 007 [arXiv:1908.02411] [INSPIRE].

[36] T.D. Blanton and S.R. Sharpe, *Alternative derivation of the relativistic three-particle quantization condition*, *Phys. Rev. D* **102** (2020) 054520 [arXiv:2007.16188] [INSPIRE].

[37] T.D. Blanton and S.R. Sharpe, *Equivalence of relativistic three-particle quantization conditions*, *Phys. Rev. D* **102** (2020) 054515 [arXiv:2007.16190] [INSPIRE].

[38] M.T. Hansen, F. Romero-López and S.R. Sharpe, *Generalizing the relativistic quantization condition to include all three-pion isospin channels*, *JHEP* **07** (2020) 047 [*Erratum ibid.* **02** (2021) 014] [arXiv:2003.10974] [INSPIRE].

[39] T.D. Blanton and S.R. Sharpe, *Relativistic three-particle quantization condition for nondegenerate scalars*, *Phys. Rev. D* **103** (2021) 054503 [arXiv:2011.05520] [INSPIRE].

JHEP09(2022)232

[40] L. Lellouch and M. Lüscher, *Weak transition matrix elements from finite volume correlation functions*, *Commun. Math. Phys.* **219** (2001) 31 [hep-lat/0003023] [INSPIRE].

[41] T. Luu and M.J. Savage, *Extracting Scattering Phase-Shifts in Higher Partial-Waves from Lattice QCD Calculations*, *Phys. Rev. D* **83** (2011) 114508 [arXiv:1101.3347] [INSPIRE].

[42] F.X. Lee, A. Alexandru and R. Brett, *Validation of the finite-volume quantization condition for two spinless particles*, arXiv:2107.04430 [INSPIRE].

[43] K. Huang and C.N. Yang, *Quantum-mechanical many-body problem with hard-sphere interaction*, *Phys. Rev.* **105** (1957) 767 [INSPIRE].

[44] S.R. Beane, W. Detmold and M.J. Savage, *n-Boson Energies at Finite Volume and Three-Boson Interactions*, *Phys. Rev. D* **76** (2007) 074507 [arXiv:0707.1670] [INSPIRE].

[45] M.T. Hansen and S.R. Sharpe, *Perturbative results for two and three particle threshold energies in finite volume*, *Phys. Rev. D* **93** (2016) 014506 [arXiv:1509.07929] [INSPIRE].

[46] M.T. Hansen and S.R. Sharpe, *Threshold expansion of the three-particle quantization condition*, *Phys. Rev. D* **93** (2016) 096006 [*Erratum ibid.* **96** (2017) 039901] [arXiv:1602.00324] [INSPIRE].

[47] F. Müller, T. Yu and A. Rusetsky, *Finite-volume energy shift of the three-pion ground state*, *Phys. Rev. D* **103** (2021) 054506 [arXiv:2011.14178] [INSPIRE].

[48] NPLQCD and QCDSF collaborations, *Charged multihadron systems in lattice QCD+QED*, *Phys. Rev. D* **103** (2021) 054504 [arXiv:2003.12130] [INSPIRE].

[49] J.-Y. Pang, J.-J. Wu, H.W. Hammer, U.-G. Meißner and A. Rusetsky, *Energy shift of the three-particle system in a finite volume*, *Phys. Rev. D* **99** (2019) 074513 [arXiv:1902.01111] [INSPIRE].

[50] F. Romero-López, A. Rusetsky, N. Schlage and C. Urbach, *Relativistic N-particle energy shift in finite volume*, *JHEP* **02** (2021) 060 [arXiv:2010.11715] [INSPIRE].

[51] Wolfram Research, Inc., *Mathematica, Version 13.0.0*.

[52] D.M. Grabowska and M.T. Hansen, *Mathematica notebook for: Analytic expansions of multi-hadron finite-volume energies: I. Two-particle states*, Zenodo, (2022) [DOI].

[53] D.C. Moore and G.T. Fleming, *Angular momentum on the lattice: The Case of non-zero linear momentum*, *Phys. Rev. D* **73** (2006) 014504 [*Erratum ibid.* **74** (2006) 079905] [hep-lat/0507018] [INSPIRE].

[54] J.J. Dudek, R.G. Edwards and C.E. Thomas, *S and D-wave phase shifts in isospin-2 $\pi\pi$ scattering from lattice QCD*, *Phys. Rev. D* **86** (2012) 034031 [arXiv:1203.6041] [INSPIRE].

[55] H.B. Meyer, *Lattice QCD and the Timelike Pion Form Factor*, *Phys. Rev. Lett.* **107** (2011) 072002 [arXiv:1105.1892] [INSPIRE].

[56] D. Bernecker and H.B. Meyer, *Vector Correlators in Lattice QCD: Methods and applications*, *Eur. Phys. J. A* **47** (2011) 148 [arXiv:1107.4388] [INSPIRE].

[57] M.T. Hansen and A. Patella, *Finite-volume effects in $(g-2)_\mu^{HVP,LO}$*, *Phys. Rev. Lett.* **123** (2019) 172001 [arXiv:1904.10010] [INSPIRE].

[58] M.T. Hansen and A. Patella, *Finite-volume and thermal effects in the leading-HVP contribution to muonic $(g-2)$*, *JHEP* **10** (2020) 029 [arXiv:2004.03935] [INSPIRE].

JHEP09(2022)232

[59] M.T. Hansen, H.B. Meyer and D. Robaina, *From deep inelastic scattering to heavy-flavor semileptonic decays: Total rates into multihadron final states from lattice QCD*, *Phys. Rev. D* **96** (2017) 094513 [arXiv:1704.08993] [INSPIRE].

[60] J. Bulava and M.T. Hansen, *Scattering amplitudes from finite-volume spectral functions*, *Phys. Rev. D* **100** (2019) 034521 [arXiv:1903.11735] [INSPIRE].

[61] M. Hansen, A. Lupo and N. Tantalo, *Extraction of spectral densities from lattice correlators*, *Phys. Rev. D* **99** (2019) 094508 [arXiv:1903.06476] [INSPIRE].

[62] P. Gambino and S. Hashimoto, *Inclusive Semileptonic Decays from Lattice QCD*, *Phys. Rev. Lett.* **125** (2020) 032001 [arXiv:2005.13730] [INSPIRE].

[63] M. Bruno and M.T. Hansen, *Variations on the Maiani-Testa approach and the inverse problem*, *JHEP* **06** (2021) 043 [arXiv:2012.11488] [INSPIRE].

[64] J. Bulava, M.T. Hansen, M.W. Hansen, A. Patella and N. Tantalo, *Inclusive rates from smeared spectral densities in the two-dimensional $O(3)$ non-linear σ-model*, *JHEP* **07** (2022) 034 [arXiv:2111.12774] [INSPIRE].

JHEP09(2022)232